Spatial Analyses of Ediacaran Communities at Mistaken Point

Emily G. Mitchell and Nicholas J. Butterfield

Department of Earth Sciences

University of Cambridge

Downing Street

Cambridge CB2 3EQ

ek338@cam.ac.uk

Abstract.— Bedding plane assemblages of Ediacaran fossils from Mistaken Point, Newfoundland, are among the oldest known records of complex multicellular life on Earth (~565 Ma). The in-situ preservation of these sessile, but otherwise deeply enigmatic organisms means that statistical analyses of specimen positions can be used to illuminate their underlying ecological dynamics, including the interactions between taxa.

Fossil assemblages on Mistaken Point D and E surfaces were mapped to millimetre accuracy using differentiated GPS. Spatial correlations between ten well defined taxa (*Bradgatia*, Charniid, *Charniodiscus*, *Fractofusus*, Ivesheadiomorphs, Lobate Discs, *Pectinifrons*, *Plumeropriscum*, *Hiemalora* and *Thectardis*), were identified using Bayesian Network Inference (BNI), and then described and analysed using Spatial Point Process Analysis. BNI found that the E surface community had a complex web of interactions and associations between taxa, with all but one taxon (*Thectardis*) interacting with at least one other. The unique spatial distribution of *Thectardis* supports previous, morphology-based arguments for its fundamentally distinct nature. BNI revealed that the D surface community showed no inter-specific interactions or associations, a pattern consistent with a homogeneous environment.

On the E surface, all six of the abundant taxonomic groups (*Fractofusus*, *Bradgatia*, Charniid, *Charniodiscus*, *Thectardis* and *Plumeropriscum*) were each found to have an unique set of interactions with other taxa, reflecting a broad range of underlying responses. Four instances of habitat associations were detected between taxa, of which two (*Charniodiscus* - *Plumeropriscum*, and *Plumeropriscum* - *Fractofusus*) led to weak competition for resources. One case of pre-emptive competition between Charniid and Lobate discs was detected. There were no instances of inter-specific facilitation. Ivesheadiomorphs interactions mirror those of

Fractofusus and *Charniodiscus*, identifying them as a form-taxonomic grouping of degradationally homogenized taphomorphs. The absence of increased fossil abundance in proximity to these taphomorphs argues against scavenging/saprophytic behaviours dominating the E surface community.

Emily G. Mitchell (ek338@cam.ac.uk) and Nicholas J. Butterfield (njb1005@cam.ac.uk).
Department of Earth Sciences, University of Cambridge. Downing Street, Cambridge CB2 3EQ, UK.

Introduction

Ediacaran organisms occupy a key place in the evolution of life on Earth, occupying the transition from the microbially-dominated world of the Proterozoic to the animal-dominated world of the Phanerozoic. Ediacaran macrofossils are represented by three broadly delineated assemblages (Waggoner 2003), of which the oldest, the Avalonian assemblage, consists of a diverse range of deep-water, sessile organisms (Narbonne 2004). Avalonian organisms share few features with living forms, making their biology, phylogenetic relationships and ecological interactions difficult to assess (Brasier et al. 2012; Hoyal Cuthill and Conway Morris 2014; Liu et al. 2015; Dufour and McIlroy 2017). Even so, almost all of these Avalonian macro-organisms were sessile (Seilacher et al. 2005, Liu et al. 2011), so their typically *in situ* preservation provides a direct account of their biological and ecological processes. Significant insights into Avalonian community ecology have been gained from the statistical analysis of specimen positions using Spatial Point Process Analyses (SPPA), with Clapham et al. (2003) demonstrating their non-random distribution on the seven principal surfaces at Mistaken Point, SE Newfoundland. More recent work has used computational and mathematical advances in SPPA to tease out the underlying biological processes, including distinctive modes of reproduction (Mitchell et al. 2015).

Almost all spatial analyses of Avalonian communities to date have focussed on interactions within a single taxon. Real organisms, however, rarely act in isolation, so any useful resolution of Avalonian ecology will also need to assess interactions *between* co-occurring taxa. The extent to which these interactions impact community structure depends on a multitude of interlinked factors, including resource availability and the response of constituent taxa to local conditions. Such interactions can be positive, where one taxon facilitates the survival of another, or negative

where one taxon inhibits another through competition, predation or chemical exclusion. Combinations of positive and negative inter-specific interactions also occur, acting over different temporal and/or spatial scales.

Recent advances of SPPA have demonstrated rich potential to resolve such relationships for communities of sessile organisms (e.g. Wiegand et al. 2007A; Muko et al. 2014). Community-scale spatial distributions depend on the interplay of a number different factors, most importantly physical environment (Wiegand et al. 2007B), organism dispersal/reproduction (Seidler and Plotkin 2006), competition for resources (Getzin et al. 2006), facilitation between taxa (Lingua et al. 2008), and differential mortality (Getzin et al. 2008). The emergent spatial patterns are rarely discernible to the naked eye (Illian et al. 2008), but can be readily resolved statistically. The distance metric used by Clapham et al. [2003] to analyse Avalonian community structure was 'nearest neighbour analysis,' where the distance from one specimen to another is measured and plotted on a cumulative frequency curve. Such calculations, however, only capture local associations, and overlook more complex or larger-scale spatial patterns: if all specimens occur within 10 cm of each other, for example, then no patterns larger than 10 cm will be detected. Nearest neighbour analyses also fail to distinguish different types of aggregation, such as those due to vegetative reproduction (e.g., stolon-like clustering) versus small-scale habitat preference (Mitchell et al. 2015. More generally, model comparisons using nearest neighbour distances are challenged by the difficulty of visualising the distribution shape or magnitude.

In contrast to nearest neighbour analysis, pair correlation functions (PCFs) describe complex spatial distributions over large distances, providing an "organism's point of view" of the surrounding community – by quantifying how density changes with increasing distance from

91 the average specimen (Law et al. 2009). In addition to within-taxon or 'univariate' analyses
92 (e.g., Mitchell et al. 2015), PCFs can be used to describe how the spatial density of one taxon
93 changes relative to another – 'bivariate' PCFs. Distinct modes of inter-specific interaction can
94 be detected as non-random distributions between taxa either as aggregation/clustering (closer
95 together than complete spatial randomness, CSR), segregation (further apart than CSR) or some
96 combination of these patterns (e.g., segregated clusters). This property means that bivariate
97 PCFs provide a description of the scale, magnitude and shape of inter-specific spatial
98 distributions, capturing complex patterns across a wide range of spatial scales. Comparison of
99 different spatial models (model fitting analyses) can be performed using Monte Carlo
100 simulations and goodness-of-fit tests to compare how well they fit observed data (Diggle 2003;
101 Illian et al. 2008). If the model fits the data well (i.e. if the goodness-of-fit test p-value,
102 p_d<0.05), the hypothesized process is strongly supported. Further information can be teased
103 from spatial patterns using Random Labelling Analyses (RLA) to assess the relative differences
104 of density-dependent behaviour between taxa pairs. Because inter-specific interactions
105 collectively define community structure, they can also be used to address how a community
106 develops from initial colonization to mature community – succession – and how different taxa
107 affect the community as a whole.
108 Not every correlation is causal of course, so demonstration of interspecific associations
109 does not in itself translate to (direct) ecological interaction. In modern systems, indirect
110 correlations can be distinguished from direct interactions by analysing the dynamics of the whole
111 system using Bayesian Network Inference (BNI) (e.g., Milns et al. 2010) – where the joint
112 probability distributions between variables (here the densities of each taxa population) is
113 represented graphically (see Milns et al. 2010 Appendix B for a Bayesian network overview).

Once direct links between taxa have been established using BNI, the nature of those links can then be investigated using bivariate SPPA. Deployed in tandem, BNI and SPPA offer a powerful means of reconstructing ecological structure from spatial data. In this study, we apply it to the question of Avalonian community ecology.

Materials and Methods

In order to assess the interspecific dynamics of Ediacaran Avalonian communities, we carried out a detailed BNI and SPPA of the D and E surfaces of the Mistaken Point Formation on SE Newfoundland (Fig. 1). These two surfaces host the most abundant and best-preserved communities of Avalonian macrofossils on record (Liu et al. 2015), dated to 565 ±3 Ma, (Benus et al. 1988). The fossils are preserved as external moulds in siltstone hemipelagites, cast from above by volcaniclastic deposits (Wood et al. 2003; Ichaso et al. 2007). This study uses the dataset of Mitchell et al. (2015), comprising 2977 fossil specimens from the 'E' surface and 1402 specimens from the 'D' surface (Supplementary Figure S1). The mean accuracy of the GPS co-ordinates of the data was 0.460 ± 06 cm horizontally and 0.8260 ± 11 cm vertically. All fossils with a consistently recognizable form were assigned to the ten taxonomic groupings (cf., Clapham et al. 2003): *Bradgatia*, Charniid, *Charniodiscus*, *Fractofusus*, *Hiemalora*, Ivesheadiomorphs, Lobate Discs, *Pectinifrons*, *Plumeropriscum* and *Thectardis*. For completeness, all remaining specimens were placed in one of two "bin groups": Holdfast Discs and Other Species (see Supplementary Figure S2 and Section S1 for taxonomic definitions).

Spatial Analyses Performed on the D and E Surfaces at Mistaken Point

Two types of spatial analyses were performed on the spatial data of the D and E surfaces: Bayesian network inference (BNI) followed by Spatial point process analyses (SPPA; see Supplementary Section S2 for extended methods). Performing BNI prior to SPPA analyses ensures that a bivariate correlations are not incorrectly linked to an inter-specific ecological process, by distinguishing a connected series of indirect correlations between several taxa from one direct correlation between two taxa. In contrast, both univariate PCF analyses and bivariate analyses between different size-classes will not suffer from this type of indirect correlation, so do not require BNI. In theory, careful bivariate SPPA should be able to distinguish direct from indirect correlations. However, when dealing with problematic fossils, such as those of the Ediacaran Avalon, BNI provides a key check on whether the signals found are indeed genuine direct correlations.

Bayesian network inference. – The set of correlations or 'edges' between taxa pairs (networks) for both D and E surfaces were identified using BNI (Heckerman et al. 1995). To find the best-fit network for each surface, the mapped areas were first divided into quadrats and discretised into zero, low and high densities. 100 samples then were created by bootstrapping (sub-sampling) these quadrat datasets at the 95% level (Magurran 2013) and the Bayesian network calculated using the software Banjo (Smith et al. 2006). The resulting set of edges formed a bimodal distribution, represented by either rare-low occurrences or high occurrences. High occurrence edges (determined using Mclust; Fraley et al. 2012) are the constituent edges of the underlying network, while the low occurrence edges are random "noise" so do not correspond to actual correlations (cf., Yu et al. 2004), with the results depicted in the form of network diagrams. The Interaction Strength is defined as the relative weight or strength of each high

occurrence edge output by Banjo, where 1 represents a strong positive correlation, -1 is a very strong negative correlation, and 0 is a non-monotonic correlation (i.e., positive and negative at different spatial scales). Where a correlation between taxa was asymmetric (i.e., the strength and/or nature of one taxon on the other was not identical), this correlation was indicated on the network diagram by an arrow. Mann-Whitney tests were used to compare the effects of taxon, edge removal and directionality, and to assess the relative importance of each to the network.

Spatial Point Process Analyses. – Unlike the BNI assessment of whole-community structure, PCF analyses can only consider individual taxon (univariate) or pairs of taxa (bivariate) during one set of analyses. To describe an entire community structure, all individuals within the community need to be accounted for, hence the inclusion of obvious organ-taxa (*Hiemalora*) and bin groups (Holdfast Discs and Other Species) in the BNI analyses. At the same time, however, the taxonomic indeterminacy of such groups is likely to obscure any palaeoecological signal based on their spatial distributions. As such, these groups have been omitted from follow-up PCF analyses and discussion. Putative taphomorph taxa, which may include the carcasses and resultant decay-induced microbial colonies (cf., Darroch et al. 2013), such as Ivesheadiomorphs and Lobate Discs are included in the PCF analyses because they are both morphologically and taphonomically distinct from all of the other taxonomic groups. Form-taxonomic groups that are likely to include a range of "natural" taxa (e.g., Holdfast Discs, Other Species, *Hiemalora*) do not have equivalent extant ecological models with which to interpret the correlations, so are excluded from the bivariate PCF analyses.

Initial data exploration and heterogeneous Poisson modelling was performed in R using the package spatstat (Baddeley et al. 2015; Supplementary Methods S2). Three types of SPPA were

used to determine the most likely underlying process behind each inter-specific interaction found using BNI: 1) pair correlation functions (PCFs); 2) model fitting to the PCFs and 3) random labelling analyses (RLAs). Programita was used to find PCFs and to perform aggregation model fitting (Wiegand and Moloney 2013; Wiegand et al. 2004, 2006, 2009). Monte Carlo simulations and Diggle's goodness-of-fit test were used to compare the fit of different spatial model PCFs to the observed PCFs (the p-value p_d, in which p_d =1 indicates a complete model fit, and p_d =0 indicates no fit [Diggle 2003; Illian et al. 2008]), and to determine the occurrence of habitat associations, competition and facilitation between taxa pairs. Note that the p_d is not a probability, but more akin to the coefficient of determination (R^2) in a linear regression wherein the value represents the percentage of the data described by the model. Finally, RLAs were used to detect density-dependent mortality processes (Jacquemyn et al. 2010; Raventós et al. 2010) using Monte Carlo simulations and calculating the difference in the extent to which each taxon departs from random labelling; i.e., whether the two populations exhibit density dependence. Because this measure is a difference between two PCF quotients, $p_d^{\mathrm{RLA}} = 0$ corresponds to a random RLA pattern between the two taxa, indicating no density dependence; by contrast, $p_d^{\mathrm{RLA}} = 1$ indicates no distribution overlap and spatial patterning that is fully density dependent. These spatial analyses and their relationships to ecological processes are outlined below; the underlying mathematics is described in detail by Wiegand and Moloney [2004] and Wiegand et al. [2004, 2006].

Using SPPA to detect and describe inter-specific interactions

In the case of sessile communities, there are just four principal inter-specific processes that influence inter-specific distributions: (1) habitat associations (co-location of two taxa on the

same habitat), (2) competition (one or both taxa limit a mutual resource), (3) facilitation (one taxon enhances the survival of another) and (4) differential mortality/density dependent effects (Wiegand et al. 2007A). Each of these processes is best described by a distinct spatial point process model, so comparison of observed bivariate spatial distributions to these models can resolve the underlying process(es) (Diggle 2003; Wiegand and Moloney 2004). Although these models have been developed primarily in the context of terrestrial forest ecology, the underlying principles are equally applicable to other communities of sessile organisms including fungal sporocarps (e.g., Liang et al. 2007) and non-motile animals (e.g. Muko et al. 2014).

Bivariate or pairwise PCFs describe how the densities between specimens belonging to two different taxa change with spatial scale, thus capturing inter-specific patterns. A bivariate PCF = 1 corresponds to two populations which exhibit complete spatial randomness (CSR) with respect to one another; i.e., they have no pairwise spatial structure and their bivariate distribution can be modelled by a homogeneous Poisson process (Illian et al. 2008). Accordingly, if a homogeneous Poisson model is the best fit to the data (i.e., exhibits CSR), then the constituent organisms do not exhibit any significant interactions. Insofar as most co-occurring taxa in most ecosystems are likely to exhibit some degree of interaction, sessile communities with no spatial structure are unusual, typically seen only during early establishment, and/or when resources are unlimited (e.g. Grieg-Smith 1979; Lin et al. 2011; Wiegand et al. 2012).

By contrast, a bivariate PCF $\neq 1$ indicates statistically significant aggregation (PCF > 1) or segregation (PCF < 1) between taxa. The magnitude of the PCF reflects the intensity of underlying biological and physical processes: two taxa populations with a PCF = 4, for example, are four times more aggregated than if they exhibited CSR; thus, the relative magnitudes of the PCFs can be used to compare relative strengths of interactions and associations.

228 *Habitat associations.* – Habitat associations occur when two (or more) taxa have the same
229 environmental preferences, such as the aggregation of alpine tree species at a common altitude
230 (Wang et al. 2011), or aggregations around a patchy distribution of soil nutrients (John et al.
231 2007). Where inter-specific interactions derive from such habitat associations, they can be
232 modelled by shared source models (also called shared parent models) where the two sets of taxa
233 aggregate around the same set of mutually exclusive points; i.e., the focus of the taxa clusters are
234 points that are not biological taxa, but some other 'environmental' factor (Wiegand et al. 2007a).
235 Where habitat associations are shared between more than two taxa, they can be described by
236 heterogeneous Poisson models, whereby specimen density is modelled by a random process in
237 which density varies across the sample area depending on the given variable (e.g. altitude).
238 Differing sensitivities to habitat heterogeneities can be encapsulated by using differing radii to
239 form the heterogeneous Poisson model that describes the habitat (Supplementary Appendix: S2).
240 Use of smaller radii to form the heterogeneous background corresponds to a stronger (more
241 sensitive) reaction to the habitat, while larger radii correspond to a weaker (more diffuse)
242 reaction. Heterogeneous habitats formed from different substrate variations are quantified by
243 different parameters of the bivariate shared source model such as the mean patch/cluster radius,
244 the total number of patches/clusters, and the mean number of specimens within each
245 patch/cluster. When two bivariate models have different parameterizations, two distinct
246 underlying substrate variations will have been identified, a reflection of ecological differences
247 between the associated taxa.
248
249 *Competition between taxa.* – Among sessile organisms, competition over limited resources is
250 typically expressed in the form of reduced specimen density, a process known as thinning. In

forests, thinning of fast growing but shade intolerant pioneer species occurs as a consequence of progressive light competition (Getzin et al. 2006). In spatial terms, such inter-specific competition is detected as segregation between taxa, where the segregation is demonstrably not due to an association with a habitat that is itself patchy (in which case the pattern would fit a bivariate shared source or heterogeneous Poisson model; see Wiegand et al. 2007a).

Inter-specific competition is scale-dependent, with pre-emptive and interference competition acting on smaller spatial scales, and resource competition acting over larger spatial scales. In modern corals, for example, segregation often occurs when one taxon excludes another by pre-emptively occupying substrate space, yielding a system where the size of individual coral heads corresponds to local levels of (pre-emptive) competition (McCook et al. 2001). In this case the pattern can be recognized spatially by small-scale thinning or segregation, which occurs at similar magnitudes to the occupying taxon. At larger scales, however, such direct inter-specific competition may derive from the release of inhibitory chemicals (allelopathy), disabling the settlement and/or survival of their neighbours yielding a quantitatively distinct spatial distribution (Willis 2007). By assessing small-scale segregation in the context of body-size, it is possible to distinguish these distinct types of competition. Large-scale segregation can be distinguished from mutual association over a habitat of segregated patches by assessing whether heterogeneous Poisson models (i.e. local habitat heterogeneities) can be used to describe the large-scale segregations (Wiegand et al. 2007b). Thus, comparison of the spatial scales of segregations and of segregated distributions with heterogeneous Poisson and shared source models (to detect habitat associations) can be used to detect competition and infer the most underlying process.

Facilitation. – Inter-specific facilitation is a process whereby the presence of one taxon benefits the survival of another (e.g. Brooker et al. 2008). Facilitation can be physical, such as protection from harsh conditions or the creation of suitable habitat (Jones et al. 1997), or intimately biotic as encountered in mutualistic endosymbioses (e.g., Bruno and Bertness 2001). In spatial terms, facilitation is indicated when the best-fit bivariate is a linked-cluster or double-cluster model (also known as bivariate Neymann-Scott/Thomas cluster models). In linked-cluster models, the spatial pattern is described by a series of clusters with normally-distributed densities (i.e., Thomas Clusters) centred on the positions of the facilitating taxa (Dickie et al. 2005; Dale and Fortin 2014). A linked Thomas double-cluster pattern is induced when the facilitated taxon (which forms Thomas Clusters around the facilitating taxon) reproduces to form secondary Thomas Clusters, resulting in Thomas double-clusters each centred on specimens of the facilitating taxon. Mutualisms are best modelled by heterogeneous Poisson process with a density created from the joint density of the two taxa, which indicates mutual clustering with no external driving factor.

Density dependent mortality processes. – Mortality rates within a population can vary due to a variety of density dependent processes, potentially influencing community spatial distributions and structure. For example, the high biodiversity of tropical forests appears to be maintained through Janzen–Connell effects, whereby taxon-specific consumers such as herbivores or pathogens generate (positive) density-dependent mortality of their prey taxa. Janzen-Connell effects prevent any single taxon from dominating the community, thus maintaining high community diversity (Velázquez et al. 2015). Mortality processes can be investigated using random labelling analyses (RLAs; Goreaud and Pélissier 2003; Raventós et al. 2010), where the

297 spatial positions of the organisms are held constant, but a specimen property such as size-class or
298 preservation detail is randomly shuffled among the observed spatial positions using Monte Carlo
299 simulations. If the observed pattern falls outside this generated simulation envelope, then the
300 specimen property (sub-group) is non-randomly distributed within the community population
301 and a density-dependant process is detected. RLAs have been used to interrogate the effects of
302 fire and canopy gaps on forest ecosystems and post-fire succession (De Luis et al. 2008; Getzin
303 et al. 2008). They can also be employed to compare the spatial distributions of superficially
304 distinct forms, such as juveniles or differentially degraded carcasses.
305 Application of SPPA to Identify Taphomorphs
306 Identification of taphomorphs is crucial to ensure an accurate ecological understanding of
307 Avalonian communities, ensuring that any impact of time-averaging can be identified and the
308 relative importance of decay-based processes assessed. Unlike extant communities, where living
309 and dead specimens are easily distinguished, identifying preserved taphomorphs is impeded
310 within Avalonian communities because the distinction between true morphological characters
311 and taphonomically degraded characters is not well defined (e.g. Antcliffe et al. 2015) and more
312 generally Avalonian morphological characters are limited in number compared to Phanerozoic
313 organisms (e.g. Dececchi et al. 2017). However, comparison of the bivariate spatial distributions
314 of putative taphomorphs with those of non-taphomorph taxa can be used to establish both the
315 likelihood of taphomorphic affinity and, for taphomorphs, their precursor taxa, where the spatial
316 distributions of taphomorph taxa is expected to mirror that of their precursor taxa, i.e., is non-
317 unique. Note that these analyses assume that there is no small-scale patchy degradation (reflected
318 by intra-specific segregation), a pattern that is not encountered on the D or E surfaces (Mitchell
319 et al. 2015). In this context, taphomorphs are are expected to exhibit a random distribution

within their precursor taxon populations, and have similar bivariate correlations. The ecological interpretations of taphomorph distributions need to keep their affinity in mind because, when taphomorphs mirror the spatial distributions of their precursors, a competitive-type spatial distribution could be detected, for example, not because the taphomorphs are directly competing with another taxon, but because the precursor taxon to the taphomorph did compete with that taxon.

Ivesheadiomorphs and Lobate Discs (Supplementary Figure S2 J, F) are the two dominant putative taphomorphs found within Mistaken Point communities (Clapham et al. 2003). Ivesheadiomorphs are characterized by a lack of consistent internal or external form, low preservation detail and rarity of symmetrical features (Liu et al. 2011). Lobate discs are also relatively irregular compared to other taxonomic groups such as the rangeomorphs, but they are characterized by a circular shape, with high relief, approximately radially symmetrical, irregular lobes. Both putative taphomorphs have a high morphological variability within identified specimens, which, when coupled with differences in spatial distributions due to the differing impact of local habitat heterogeneities and/or differing times of community developments, means that their affinities should be assessed on a surface by surface basis. Therefore, any taphomorph and their precursor taxa identified on one surface may not apply to another (Kenchington and Wilby 2015).

Results and Discussion

Our analyses focussed on the D and E surface communities of Mistaken Point, Newfoundland. The E surface is the most diverse and abundant assemblage of Avalonian fossils on record, preserving 14 distinct species (with eight abundant taxa) and 2977 identifiable

specimens within its 63.5 m^2 area (Clapham et al. 2003, Mitchell et al. 2015). The Mistaken Point D surface is also taxonomically diverse, preserving eight identifiable species (with three abundant taxa) within its 62.0 m^2 area and 1402 individual fossils. Combined BNI and advanced SPPA revealed an unprecedented level of ecological insight of the two principle surfaces, and reveal ecological distinctions between them beyond differences in community composition (cf., Clapham et al. 2003).

BNI

E surface. – On the E surface, BNI analysis revealed a complex network of inter-specific interaction and associations between the 12 taxonomic groups identified in this study (Fig. 2). Out of a possible 66 correlations, we identified 14 inter-specific correlations involving all but one of the constituent taxa, *Thectardis*. On average, each taxon interacted with at least two other taxa (2.41 mean per-taxon correlation); though interaction strengths were skewed towards low values (0.17 mean Interaction Strength). There were four non-monotonic correlations (different positive and negative correlations at different spatial scales), one negative correlation and nine positive correlations (Table 1). *Fractofusus* and *Plumeropriscum* were the most connected taxa, with four correlations each: *Fractofusus* correlated with *Plumeropriscum*, Ivesheadiomorphs, Lobate Discs and Holdfast Discs; *Plumeropriscum* correlated with *Fractofusus*, *Charniodiscus*, Holdfast Discs and Other Species. *Bradgatia* was the least connected taxon within the network, only correlating with the Charniid group. Excluding *Hiemalora* and the two bin groups resulted in eight inter-specific correlations among the eight remaining taxa – with a mean per taxon correlation of 2.28 and a mean Interaction Strength of 0.19.

364 The only taxon on the E surface to show no inter-specific interactions nor associations was
365 *Thectardis* (based on 10,000,000 networks from 100 95% bootstrap samples, Fig. 2), which
366 could be selectively excluded from the analyses without changing the network (*p = 0.54;* Fig. 2;
367 Table 1). This result is not due to its low abundance (< 1% of E surface specimens): the BNI
368 data are input using discrete values, so the absolute abundance does not influence the network
369 output. Moreover, taxa with similar abundances (*Hiemalora* and *Bradgatia*) interact with other
370 taxa even at the lower sampling of 80% BNI (Table 1). As such, the absence of *Thectardis* from
371 the recovered network is most likely to be a real ecological signal, demonstrating its ecological
372 isolation from other E surface taxa. In addition to its conspicuously unconnected spatial
373 distribution, *Thectardis* also stands out morphologically, distinguished by a simple triangular
374 outline (Supplementary Figure S3D) and absence of the fractal or frondose differentiation seen in
375 most co-occurring forms. Sperling et al. (2011) have speculated on its possible sponge
376 affiliations, but with little corroborating evidence (Antcliffe et al. 2011). The ecological
377 disparity of *Thectardis* is consistent with a different feeding mode of *Thectardis* to the other E
378 surface taxa, for example, the active filter feeding that sponges employ, versus the passive
379 osmotrophic feeding of the Rangeomorphs. As such, our spatial analyses are consistent, but not
380 definitive, in the support of a sponge affinity of *Thectardis*.
381
382 *D surface.* – Despite its comparably abundant and diverse assemblage, BNI analysis of the D
383 surface found no bivariate correlations between the three abundant taxa (*Fractofusus*, *Bradgatia*
384 and Pectinifrons), while the remaining five (*Plumeropriscum*, *Charniodiscus*, Ivesheadiomorphs,
385 Charniid and Lobate Discs) occur in too low an abundance (< 30 specimens/taxon) to yield
386 statistically significant results. As such, there are no reportable correlations or interactions

387 strengths for D surface, and no potential for follow-up SPPA analysis. The only non-random
388 PCF distribution on D is the univariate distribution of *Fractofusus* (Mitchell et al. 2015).
389 The marked disparity in bivariate correlations between the D and E surfaces points to
390 fundamental differences in their respective community structures, though only if the respective
391 datasets are taphonomically comparable. It is notable, for example, that the overall density of
392 fossils on D surface is ~ 50% that of E surface (Clapham et al. 2003; Mitchell et al. 2015) which
393 could potentially derive from differential modern erosion (cf., Matthews et al. 2017). Our sub-
394 sampling the E surface community to a similar density as the D surface (50%), however, found
395 that three of its 14 correlations were still readily detectable (Table 1), demonstrating clear signal
396 retention. Moreover, the three abundant taxa on D surface taxa have a total density comparable
397 to that of their counterparts on E surface (2.27 - 22.40 specimens/m^2 vs. 0.62 - 20.70
398 specimens/m^2 respectively), while the E surface pairwise densities of both *Bradgatia* + Charniid
399 and Charniid + Lobate Discs are greater than the pairwise densities of D surface taxon-pairs. At
400 least in the case of these taxa and pairwise densities, it is clear that the absence of correlations on
401 D surface is not an artefact of differential preservation or sampling. The differences are
402 ecological.
403 Another possible interpretation of the disparity in BNI results between E and D is that the
404 lower specimen density of D represents an early stage of community succession, yet to put
405 pressure on local resources (Townsend et al. 2003); i.e., the organisms have not yet reached
406 sufficient densities to be impacted by each other or their habitat. The presence of at least two
407 generations of *Fractofusus* (Mitchell et al. 2015), however, demonstrates substantial community
408 development. As such, the absence of ecological interactions, or even interspecific correlation,
409 on the D surface is more likely to reflect a more homogenous background environment than that

410 of E surface, with no habitat patchiness to locally exacerbate competition. Habitat heterogeneity
411 is generally correlated to taxonomic diversity (e.g. Agarwal 2008), so the reduced diversity of
412 the D surface could be explained simply as a consequence of the homogeneous environment.
413
414 SPPA of the E surface
415 Using bivariate PCF analyses, we found seven of the eight E surface correlations to be
416 habitat associations and one the result of pre-emptive competition (Fig. 3; Supplementary Table
417 S1). Within the habitat associations, two were devoid of any discernible interaction beyond co-
418 location, three exhibited non-unique or mirrored behaviours (Supplementary Table S2), and two
419 showed clear evidence of subsequent behaviour. There was no evidence of facilitation between
420 any of the taxa on the E surface.
421
422 *Pre-emptive competition.* – Lobate Discs segregated from Charniid on spatial scales smaller than
423 0.5m at a PCF of 0.75; i.e. reducing Charniid density by 21% ($PCF_{min} = 0.79$; Fig. 3A;
424 Supplementary Table S1). This small scale segregation of Lobate Discs and Charniid is of the
425 same spatial scale as the mean radius of Lobate Discs (Clapham et al. 2003), suggesting that the
426 segregation is due to pre-emptive competition of Charniid not settling directly on the Lobate
427 Discs. An alternative taphonomic explanation, where Charniid is preferentially degraded in
428 association with Lobate Discs, is unlikely given the absence of such effects with co-occurring
429 rangeomorphs such as *Bradgatia* or *Plumeropriscum*. Allelopathy (the active release of
430 inhibitory biochemicals) also causes small-scale segregation, but in this case the Lobate Disc –
431 Charniid correlation exhibits the same spatial scale as the univariate Lobate Discs (albeit non-
432 significant) aggregation (Fig. 3A), suggesting that the underlying phenomenon did not extend

433 more broadly (as expected in with allelopathic diffusion). That said, other chemical processes
434 could result in such segregation if the inhibitory compound(s) remained localized within the
435 Lobate Disc-occupied substrate, such as the H_2S proposed by Dufour and McIlroy (2016).
436 Interpreting the mechanisms behind the Lobate Discs – Charniid segregation is
437 substantially hampered by the problematic nature of Lobate Discs, which lack a formal
438 taxonomical definition or basic biological resolution; current interpretations range from a distinct
439 macroscopic taxon to microbial colonies, taphomorphs or even sedimentary intrusions (e.g., Liu
440 et al. 2011; Laflamme et al. 2011) . Nonetheless, the statistical evidence for segregation is
441 unambiguous and demonstrates that the Lobate Discs were largely in place before Charniid
442 establishment.
443 The absence of allelopathy within the E surface community contrasts with extant marine
444 sessile communities, where such chemical-based exclusion and other direct interference
445 competition such as overgrowth competition is pervasive (e.g. Jackson et al. 1975; Engel et al.
446 2000). Modern communities of sessile deep-sea organisms also tend to be densely packed, with
447 corals and sponge commonly occupying 90% or more of available substrate (e.g. Calle 2010). By
448 contrast, even the relatively dense E surface community has conspicuously lower substrate
449 occupation rates (< 13%; Clapham et al. 2003), reflecting correspondingly lower levels of
450 substrate competition. Even so, the univariate Charniid PCF shows strong environmentally-
451 mediated spatial distributions (Supplementary Figure S3; Mitchell et al. 2015), suggesting that
452 they may be more susceptible to the local substrate differences induced by the presence of
453 Lobate Discs.
454

455 *Unique habitat associations.* – PCF analyses found that seven bivariate correlations were most
456 likely due to habitat associations, where both of the constituent taxa experienced enhanced
457 survival related to some (otherwise unseen) aspect of the background environment (Fig. 4A).
458 Two of these seven unique habitat associations resulted in large-scale aggregations (*Bradgatia* –
459 Charniid and *Fractofusus* – Lobate Discs; Fig. 3B, C), but without reducing the longer-term
460 survival of either taxon (as would have been detected by segregation in the bivariate PCFs). The
461 *Bradgatia* – Charniid correlation is a relatively consistent aggregation which corresponds to a
462 mutual density increase of Bradgatia and Charniid by 15% above CSR up to 3.4 m radius
463 (PCF_{max} = 1.15; Fig. 3B). The greatest aggregation of *Bradgatia* and Charniid occurs under 0.8
464 m radius (PCF_{max} = 1.3) and is best modelled by a shared source model (p_d = *0.66*; Fig. 3B).
465 This habitat heterogeneity also impacts Charniid, which is inferred by the similar spatial scales
466 of the aggregated part of the univariate Charniid and bivariate Charniid - *Bradgatia* spatial
467 distributions, but only very weakly affects *Bradgatia* given the random univariate Bradgatia PCF
468 (Fig 3A - C). The Charniid - *Bradgatia* spatial pattern is much weaker than that of the univariate
469 Charniid aggregation, suggesting that this habitat heterogeneity strongly promotes Charniid
470 establishment and only weakly promotes *Bradgatia* establishment. A similar pattern is observed
471 in corals where settlement is dependent on the type of previously established algae (cf., Carlon
472 and Olson 1993). Univariate Charniid and the bivariate Charniid - *Bradgatia* are the only PCFs
473 that correlate at this spatial scale (Fig. 3A-C), suggesting that this metre-scale habitat
474 heterogeneity did not affect other taxa.
475 The E surface *Fractofusus* – Lobate Discs correlation is consistent but weak (PCF_{max}=
476 1.15) up to a 2 m radius between the taxa; it is best modelled by a shared source model (p_d =
477 0.70, Fig. 3C). The association between *Fractofusus* and Lobate Discs does not exhibit the same

478 spatial scaling as other univariate or bivariate spatial distributions (Fig. 3A - C) and could not be
479 modelled by another best-fit bivariate model (Supplementary Table S2): it is a unique
480 association, and indicates another distinct background heterogeneity in addition to that of
481 *Bradgatia* and Charniid. Notably, this pattern is a rare instance where spatial pattern is evident in
482 the field, with *Fractofusus* commonly observed to overlie Lobate Discs (cf., Dufour and McIlroy
483 2016).
484
485 *Habitat associations leading to competition. – Plumeropriscum – Fractofusus* and
486 *Plumeropriscum – Charniodiscus* both exhibit small-scale aggregation coupled with large-scale
487 segregation (Fig. 3C). In the case of *Fractofusus* and *Plumeropriscum*, both taxa exhibit
488 increased densities over a shared paleo-environmental heterogeneity (as revealed by being best
489 modelled by a shared source $p_d = 0.79$; Fig. 3C; Supplementary Table S1), coupled with
490 segregation ($PCF_{min} = 0.92$ between 1.5 m and 3.5 m, reducing the established specimen density
491 by 8.4%, Fig. 3C). Notably, this segregation could not be modelled by a heterogeneous Poisson
492 model (Supplementary Tables S1 and S4). Such patterns most likely derive from inter-specific
493 resource competition as growth leads to progressive thinning and spatial segregation of the most
494 mature specimens (cf. Mason et al. 2003; Fig. 4A, B). This same style of habitat association and
495 resource competition is seen between *Plumeropriscum* and *Charniodiscus*, which is similarly
496 best modelled by a shared source ($p_d = 0.97$, Fig. 3C; Supplementary Table S1). The habitat
497 associations between *Plumeropriscum – Fractofusus* and *Plumeropriscum – Charniodiscus* were
498 significantly different, pointing to two distinct aggregation sources ($p_d = 0.04$ and $p_d = 0.01$,
499 Supplementary Tables S1 and S2), for example variations in microbial mat coverage or depth.

Out of a possible 13 taxon-pairs on E surface, it is notable that inter-specific resource competition is limited to just these two instances. The limited instances of inter-specific competition stand in stark contrast to extant marine benthic communities and other sessile communities (such as terrestrial forests) where competition is ubiquitous (Bertness and Leonard 1997; Wiegand et al. 2007B). These spatial differences also contrast with the suggestion that Avalonian communities are similarly structured to extant benthic communities (Clapham et al. 2003). At the same time, however, it is these three competing taxa – *Fractofusus*, *Plumeropriscum* and *Charniodiscus* – that form the majority (58.6%) of the specimens on E surface. In other words, although the majority of *taxa* do not exhibit inter-specific resource competition, the majority of *individuals* appear to be competing for limited resources.

Importance of using BNI combined with SPPA. – SPPA applied to all possible pairwise combinations on E surface revealed six non-random correlations not found by BNI. These derive from the combined effects of two unrelated correlations rather than direct interaction. Lobate Discs, for example, have a non-random PCF with respect to *Plumeropriscum*, but because this correlation was not found by BNI, the signal should be interpreted as a consequence of each taxon being separately correlated with *Fractofusus*. The presence of indirect, non-random PCFs that have a clear connection via an intermediate taxon highlights the importance of using BNI in combination with SPPA to minimise Type I errors (false positives) when drawing palaeoecological inferences.

Using spatial analyses to identify putative taphomorphs

522 The D and E surface communities contain abundant populations of Ivesheadiomorphs and
523 Lobate discs, both of which have been widely viewed as the degraded taphomorphs of more
524 'biological' taxa (Liu et al. 2011). Such interpretation clearly bears critically on any spatial
525 analysis of Avalonian ecology, particularly on the E surface, where these two problematic forms
526 represent 13.2% of all individuals, and 46.7% of the total fossil area (~ biomass) (Clapham et al.
527 2003). Our PCF and RLA analyses strongly support the identification of ivesheadiomophs as
528 taphomorphs and identify the likely precursor taxa, but find that Lobate Discs spatial
529 distributions are inconsistent with a taphomorph affinity.
530
531 *Ivesheadiomorph affinity and precursor taxa*. – PCF analyses found that *Fractofusus* –
532 Ivesheadiomorph was best modelled by a shared source model (p_d = 0.65; Fig. 3D, E;
533 Supplementary Table S1) as was *Charniodiscus* – Ivesheadiomorphs (p_d = 0.82). Neither the
534 *Fractofusus* – Ivesheadiomorph nor *Charniodiscus* – Ivesheadiomorphs best-fit models were
535 unique, and further analyses strongly suggests that *Charniodiscus* and *Fractofusus* are the
536 precursor taxa of Ivesheadiomorphs on the E surface (cf. Liu et al. 2011) as follows: First, the
537 *Fractofusus* – Ivesheadiomorph and *Charniodiscus* – Ivesheadiomorphs correlations closely
538 follow the univariate *Fractofusus* and *Charniodiscus* clustering (they exhibit the same small-
539 scale high aggregation under 0.4 m (Fig. 3E). Second, the best-fit models for both correlations
540 are heterogeneous Poisson models based on *Fractofusus* (for the Ivesheadiomorph – *Fractofusus*
541 correlation, p_d = 0.55) or *Charniodiscus* (for the Ivesheadiomorph – *Charniodiscus* correlation,
542 p_d = 0.75) densities. Likewise, the *Fractofusus* – Ivesheadiomorph distribution could be
543 modelled by the *Plumeropriscum* – *Fractofusus* correlation (p_d = 0.56) and vice versa (p_d = 0.71).
544 And finally, the RLA show that Ivesheadiomorphs are randomly distributed within both the

545 *Fractofusus* and *Charniodiscus* populations (p_d^{RLA} <0.05 for both; Fig. 3F; Supplementary
546 Table S3).
547 BNI of the E surface revealed a correlation between Ivesheadiomorphs and
548 *Plumeropriscum*, which is best modelled by a shared source model (p_d = 0.69; Fig. 3D, E;
549 Supplementary Table S1), with a large-scale segregation of 95% CSR occurring between 2.0 m
550 and 3.5 m. However, corresponding SPPA rules out any precursor-taphomorph correspondence:
551 the PCF of the Ivesheadiomorph – *Plumeropriscum* distribution differs significantly from the
552 univariate *Plumeropriscum*; the bivariate correlation of the two 'taxa' cannot be modelled as a
553 heterogeneous Poisson model using *Plumeropriscum* and RLA also shows significantly different
554 density dependant behaviour of *Plumeropriscum* relative to Ivesheadiomorphs, and there is
555 further overlap with other bivariate models (Supplementary Tables: Tables S2 and S4): the
556 Ivesheadiomorph – *Plumeropriscum* correlation can be modelled by the same best-fit model as
557 *Fractofusus* – *Plumeropriscum* (p_d = *0.58,* for non-CSR PCF) and by *Charniodiscus* –
558 *Plumeropriscum* (p_d = *0.55,* for non-CSR PCF), pointing to closely comparable bivariate habits
559 between Ivesheadiomorphs and both *Fractofusus* and *Charniodiscus* (that the combined 58% and
560 55% of these two spatial distributions exceed 100% is explained by a modest 25% overlap in the
561 two models).
562 These three Ivesheadiomorph correlations (Ivesheadiomorph - *Fractofusus*,
563 Ivesheadiomorph - *Charniodiscus* and Ivesheadiomorph - *Plumeropriscum*) are notable in being
564 the only observed correlations on the D and E surfaces that were non-unique. In other words, the
565 spatial distributions of these pair-wise correlations are statistically indistinguishable from the
566 bivariate distributions of other pairs – in marked contrast to all other non-Ivesheadiomorph
567 correlations (Supplementary Table S2). The similarity of these Ivesheadiomorph correlations

568 with other E surface correlations makes a microbial affinity (cf. Laflamme et al. 2011) unlikely.
569 Further, the inclusion of non-frondose *Fractofusus* within the Ivesheadiomorph correlations is
570 inconsistent with the interpretation of ivesheadiomorphs as sediment intrusions beneath fronds
571 (cf. Wilby et al. 2011) since there was no space between recumbent *Fractofusus* and the
572 substrate which could be infilled by sediment.
573
574 *Putative non-Ivesheadiomorph taphomorphs*. – Apart from Ivesheadiomorphs, it has been argued
575 that Lobate Discs (Liu et al. 2011), *Thectardis,* and *Charniodiscus* (Antcliffe et al. 2015) may
576 also represent preservational variants of other (mostly unspecified) entities (as opposed to organ
577 taxa, such as *Hiemalora*). Possible precursor taxa for Lobate Discs on E surface are (the
578 holdfasts of) Charniid, *Charniodiscus*, *Bradgatia* and *Plumeropriscum*. None of these exhibit
579 statistically similar bivariate spatial correlations, however, substantially undermining any
580 taxonomic connection (Fig. 3D, E). Indeed, there are no frondose taxa on E surface that could
581 have been a plausible precursor to Lobate Discs. By the same token, neither *Charniodiscus* nor
582 *Thectardis* have univariate and bivariate spatial patterns that are statistically comparable to any
583 co-occurring taxa, so are unlikely to be taphomorphic variants (contra Antcliffe et al. 2015)
584 (Mitchell et al. 2015; Fig. 2; Supplementary Figure S3; Table S2; contra Antcliffe et al. [2015]).
585
586 *Multiple successions.* – On a more general level, it is possible that the fossils preserved on any
587 particular bedding surface belong to a succession of discrete communities; i.e., not all were alive
588 at the same time (cf. Liu et al. 2012; McIlroy and Garton 2010; Antcliffe et al. 2016). The BNI
589 and SPPA results, however, are inconsistent with multiple colonization of the E surface as are
590 the univariate population analyses of Darroch et al. [2013] and SPPA of Mitchell et al. [2015]).

591 Significantly, size-distribution analyses of the E surface demonstrate single (not multiple)
592 populations of abundant taxa (with the exception of *Thectardis*; Darroch et al. 2013), and
593 univariate spatial analyses find that there is no evidence of strong univariate environmental
594 (habitat) influences in any E surface taxa except Charniid (which eliminates bivariate
595 correlations due to repeated successions being subject to the same environmental influence;
596 Mitchell et al. 2015). As such, seven of the eight E surface taxa can be recognized as
597 contemporaneous. This reasoning cannot be applied to *Thectardis* since it is not spatially
598 correlated with any other taxon; however, its shared current alignment with frondose taxa on the
599 same bedding surface suggests that it too was part of this community (Clapham et al. 2004) .
600
601 *Taphomorph ecology*. – Within Ediacaran communities, the habitat heterogeneity produced by
602 decaying organisms has been proposed as the determining factor in community structure
603 (Antcliffe et al. 2015; Budd and Jensen 2015; Liu et al. 2015; Dulfour and McIlroy 2016). In
604 this "Ediacaran-fall" model, localized concentrations of resources represented by macro-
605 carcasses are likened to more recent whale-fall or wood-fall ecosystems (c.f., Smith et al. 2015),
606 whereby decaying organisms form the focus of for colonizers to settle upon and form
607 communities. When organisms feed directly on this carbon (or indirectly on the sulphides)
608 produced by specimen decay), then the population densities of scavenger/saprophytic species
609 tend to increase around the local resource, resulting in a spatial pattern best modelled as a linked
610 cluster (or double cluster) model, or a heterogenous Poisson model based on carcass densities
611 (Wiegand and Moloney 2014). Notably, no such spatial patterns are observed with
612 Ivesheadiomorphs on the Mistaken Point surfaces. Instead there is a mutual clustering around
613 two different shared sources for Ivesheadiomorphs, one with *Fractofusus* and the other with

614 *Charniodiscus* (Fig. 3D; Supplementary Table S1); i.e., there is no increased survival for taxa
615 that settle near Ivesheadiomorphs. The correlations between Ivesheadiomorphs – *Fractofusus*
616 and Ivesheadiomorphs – *Charniodiscus* are most likely a reflection of the single taxon clustering
617 that occurs for both these taxa, with dead specimens (i.e., Ivesheadiomorphs) randomly
618 distributed amongst the living. Thus, our spatial analyses refute the hypothesis that any single
619 taxa (such as *Fractofusus, Charniodiscus* or *Plumeropriscum*) were scavengers. Alternatively,
620 a habitat heterogeneity formed from unpreserved decayed carcasses could be detected as a
621 habitat association between taxa. However, if several taxa pairs were impacted by the same
622 single decay heterogeneity, then they would be expected to share the same shared-source model
623 – inconsistent with the four distinct habitat associations present on E surface, and the absence of
624 any on the D surface. Taken together, SPPA analysis rules out saprophytic habits as a
625 controlling factor in structuring these Avalonian communities.
626

627 **Conclusions**

628 Our spatial analyses of the E surface at Mistaken Point reveal a fundamentally more
629 complex community structure than has been previously recognized (Fig. 2), showing clear
630 ecological differentiation between taxa, with all six abundant non-taphomorph taxa developing
631 different responses to a variety of habitat spatial variations (Fig. 5, Supplementary Table S2).
632 The presence of multiple ecological responses demonstrates that individual taxa have distinct
633 approaches for adapting to local habitat, leading to divergent selection, reproductive isolation
634 and ultimately biodiversification (Kawecki and Ebert 2004; Mitchell-Olds and Schmitt 2006;
635 Hereford 2009; Sobel et al. 2010; Futuyma and Agrawal 2009). The fundamentally different

636 degree of organismal interaction in these Avalonian communities demonstrates their
637 fundamentally non-uniformitarian nature, highlighted by the complete lack of D surface
638 community inter-specific interactions, and could well account for the conspicuously slow nature
639 of their evolutionary turnover (cf., Grazhdankin 2004). At the same time, the low levels of
640 competitive interactions (for example in comparison to modern forests or deep-sea reefs)
641 established in these earliest communities of macroscopic organisms sets the stage for progressive
642 escalation; first through elevated competition for resources, then leading to macroscopic
643 movement and ultimately carnivory.
644 This study has demonstrated how new approaches to spatial analysis can resolve key
645 aspects of Avalonian paleoecology. By combining BNI with PCFs it is possible to describe the
646 spatial variation of specimen densities between taxa pairs, establishing when taxa are responding
647 to each other and/or their habitat. Modelling fitting takes these analyses beyond descriptive
648 statistics, enabling verifiable predictions to be made and to test ecological hypotheses. RLA
649 enables the comparison of density dependant behaviour within a given spatial pattern, thus
650 assisting in the identification of taphomorphs. These techniques present a framework for further
651 investigations, which can incorporate morphological details such as body-size to investigate
652 broader ecological themes such as the implications of tiering and/or ecological successions on
653 Ediacaran community structure.
654
655
656
657

References

Agarwal, S. K. 2008. Fundamentals of ecology. APH Publishing.

Antcliffe, J. B., A. D. Hancy, and M. D. Brasier. 2015. A new ecological model for the ~ 565 Ma Ediacaran biota of Mistaken Point, Newfoundland. Precambrian Research 268:227–242.

Antcliffe, J. B., R. H. T. Callow, and M. D. Brasier. 2014. Giving the early fossil record of sponges a squeeze. Biological Reviews 89:972–1004.

Baddeley, A., E. Rubak, and R. Turner. 2015. Spatial point patterns: methodology and applications with R. CRC Press.

Benus, A. P. 1988. Sedimentological context of a deep–water Ediacaran fauna (Mistaken Point, Avalon Zone, eastern Newfoundland). Trace Fossils, Small Shelly Fossils and the Precambrian–Cambrian Boundary. New York State Museum and Geological Survey Bulletin 463:8–9.

Bertness, . D., and R. Callaway. 1994. Positive interactions in communities. Trends in Ecology & Evolution 9:191–193.

Brasier, M. D., and J. B. Antcliffe. 2009. Evolutionary relationships within the Avalonian Ediacara biota: new insights from laser analysis. Journal of the Geological Society 166:363–384.

Brasier, M. D., J. B. Antcliffe, and A. G. Liu. 2012. The architecture of Ediacaran fronds. Palaeontology 55:1105–1124.

Brooker, R. W., F. T. Maestre, R. M. Callaway, et al. 2008. Facilitation in plant communities: the past, the present, and the future. Journal of Ecology 96:18–34.

Bruno, J. F. 2001. Habitat modification and facilitation in benthic marine communities. Marine community ecology.

Budd, G. E., and S. Jensen. 2017. The origin of the animals and a 'Savannah' hypothesis for early bilaterian evolution. Biological Reviews 92:446–473.

681 Calle, S. R. 2010. Ecological Aspects of Sponges in Mesophotic Coral Ecosystems. *In* Masters
682 Abstracts International, vol. 49, no. 03. (Doctoral dissertation, University Of Puerto Rico).
683 Carlon, D. B., and R. R. Olson. 1993. Larval dispersal distance as an explanation for adult spatial
684 pattern in two Caribbean reef corals. Journal of Experimental Marine Biology and
685 Ecology 173:247–263.
686 Clapham, M. E., G. M. Narbonne, and J. G. Gehling. 2003. Paleoecology of the oldest known
687 animal communities: Ediacaran assemblages at Mistaken Point,
688 Newfoundland. Paleobiology 29:527–544.
689 Clapham, M. E., G. M. Narbonne, J. G. Gehling, C. Greentree, and M. M. Anderson. 2004.
690 *Thectardis avalonensis*: a new Ediacaran fossil from the Mistaken Point biota,
691 Newfoundland. Journal of Paleontology 78:1031–1036.
692 Clapham, M. E., and G. M. Narbonne. 2002. Ediacaran epifaunal tiering. Geology 30:627–630.
693 Dececchi, T. A., G. M. Narbonne, C. Greentree and M. Laflamme. 2017. Relating Ediacaran
694 Fronds. Paleobiology 43:171–180.
695 Dale, M.R. T., and M. J. Fortin. 2014. Spatial analysis: a guide for ecologists. Cambridge
696 University Press.
697 Darroch, S. A. F., M. Laflamme, and M. E. Clapham. 2013. Population structure of the oldest
698 known macroscopic communities from Mistaken Point, Newfoundland. Paleobiology 39:591–
699 608.
700 De Luis, M., J. Raventós, T. Wiegand, and J. C. González- Hidalgo. 2008. Temporal and spatial
701 differentiation in seedling emergence may promote species coexistence in Mediterranean fire-
702 prone ecosystems. Ecography 31:620–629.

703 Dickie, I. A., S. A. Schnitzer, P. B. Reich, and S. E. Hobbie. 2005. Spatially disjunct effects of
704 co-occurring competition and facilitation. Ecology Letters 8: 1191–1200.
705 Diggle, P. 2003. Statistical Analysis of Spatial Point Patterns., 2nd edn. Arnold: London.
706 Dufour, S. C. and D. McIlroy. 2017. Ediacaran pre–placozoan diploblasts in the Avalonian biota:
707 the role of chemosynthesis in the evolution of early animal life. Geological Society, London,
708 Special Publications 448:211–219.
709 Engel, S., and J. R. Pawlik. 2000. Allelopathic activities of sponge extracts. Marine Ecology
710 Progress Series 207:273–282.
711 Fajardo, A., and E. J.B. McIntire. 2010. Merged trees in second–growth, fire–origin forests in
712 Patagonia, Chile: positive spatial association patterns and their ecological
713 implications. American Journal of Botany 97:1424–1430.
714 Fraley, C., A. E. Raftery, and L. Scrucca. 2012. Normal mixture modeling for model–based
715 clustering, classification, and density estimation. Department of Statistics, University of
716 Washington 23:2012.
717 Futuyma, D. J., and A. A. Agrawal. 2009. Macroevolution and the biological diversity of plants
718 and herbivores. Proceedings of the National Academy of Sciences 106:18054–18061.
719 Getzin, S., Ch. Dean, F. He, J. A Trofymow, K. Wiegand, and T. Wiegand. 2006. Spatial
720 patterns and competition of tree species in a Douglasfir chronosequence on Vancouver
721 Island. Ecography 29:671–682.
722 Getzin, S., T. W., K. Wiegand, and F. He. 2008. Heterogeneity influences spatial patterns and
723 demographics in forest stands. Journal of Ecology 96:807–820.

724 Goreaud, F., and R. Pélissier. 2003. Avoiding misinterpretation of biotic interactions with the
725 intertype K12-function: population independence vs. random labelling hypotheses. Journal of
726 vegetation science 14,:681–692.
727 Grazhdankin, D. 2004. Patterns of distribution in the Ediacaran biotas: facies versus
728 biogeography and evolution. Paleobiology 30:203–221.
729 Greig–Smith, P. 1979. Pattern in vegetation. Journal of Ecology 67:755–779.
730 Heckerman, D., Dan G., and D. M. Chickering. 1995. Learning Bayesian networks: The
731 combination of knowledge and statistical data. Machine learning 20:197–243.
732 Hereford, J. 2009. A quantitative survey of local adaptation and fitness trade–offs. The American
733 Naturalist 173:579–588.
734 Hofmann, H. J., S. J. O'Brien, and A. F. King. 2008. Ediacaran biota on Bonavista peninsula,
735 Newfoundland, Canada. Journal of Paleontology 82:1–36.
736 Hoyal Cuthill, J. F., and S. Conway Morris. 2014. Fractal branching organizations of Ediacaran
737 rangeomorph fronds reveal a lost Proterozoic body plan. Proceedings of the National Academy
738 of Sciences 111:13122–13126.
739 Ichaso, A. A., R. W. Dalrymple, and G. M. Narbonne. 2007. Paleoenvironmental and basin
740 analysis of the late Neoproterozoic (Ediacaran) upper Conception and St. John's groups, west
741 Conception Bay, Newfoundland. Canadian Journal of Earth Sciences 44:25–41.
742 Illian, J., A. Penttinen, H. Stoyan, and D. Stoyan. 2008. Statistical analysis and modelling of
743 spatial point patterns. Vol. 70. John Wiley & Sons.
744 Jackson, J. B. C. and L. Buss. 1975. Alleopathy and spatial competition among coral reef
745 invertebrates. Proceedings of the National Academy of Sciences72:5160–5163.

746 Jacquemyn, H., P. Endels, O. Honnay, and T. Wiegand. 2010. Evaluating management
747 interventions in small populations of a perennial herb Primula vulgaris using spatio- temporal
748 analyses of point patterns. Journal of applied ecology 47:431–440.
749 John, R., J. W. Dalling, K. E. Harms, et al. 2007 Soil nutrients influence spatial distributions of
750 tropical tree species. Proceedings of the National Academy of Sciences 104:864–869.
751 Jones, C. G., J. H. Lawton, and M. Shachak. 1997. Positive and negative effects of organisms as
752 physical ecosystem engineers. Ecology 78:1946–1957.
753 Kawecki, T. J., and D. Ebert. 2004. Conceptual issues in local adaptation. Ecology
754 letters 7:1225–1241.
755 Kenchington, C. G. and P. R Wilby. 2014. Of time and taphonomy: preservation in the Ediacaran
756 *in* Reading and writing of the fossil record: Preservational pathways to exceptional fossilization,
757 The Paleontological Society Papers, 20, pp. 101–122.
758 Laflamme, M., J. D. Schiffbauer, and G. M. Narbonne. 2011. Deep-water microbially induced
759 sedimentary structures (MISS) in deep time: The Ediacaran fossil Ivesheadia. Microbial mats in
760 siliciclastic depositional systems through time. SEPM Special Publication 101:111–123.
761 Law, R., J. Illian, D. F. R. P. Burslem, G Gratzer, C. V. S. Gunatilleke, and I. A. U. N.
762 Gunatilleke. 2009. Ecological information from spatial patterns of plants: insights from point
763 process theory. Journal of Ecology 97:616–628.
764 Li, L., W. H. Ye, S. G. Wei, J. Y. Lian, and Z. L. Huang. 2014. Spatial patterns and associations
765 between species belonging to four genera of the Lauraceae family. PloS one 9:e111500.
766 Li, L., Z. Huang, W. Ye, et al. 2009. Spatial distributions of tree species in a subtropical forest of
767 China. Oikos 118:495–502.

768 Liang, Y., L. D. Guo, X. J. Du, and K. P. Ma. 2007. Spatial structure and diversity of woody
769 plants and ectomycorrhizal fungus sporocarps in a natural subtropical forest. Mycorrhiza 17:271.
770 Lingua, E., P. Cherubini, R. Motta, and P. Nola. 2008. Spatial structure along an altitudinal
771 gradient in the Italian central Alps suggests competition and facilitation among coniferous
772 species. Journal of Vegetation Science 19:425–436.
773 Liu, A. G., C. G. Kenchington, and E. G. Mitchell. 2015. Remarkable insights into the
774 paleoecology of the Avalonian Ediacaran macrobiota. Gondwana Research 27:1355–1380.
775 Liu, A. G., D. Mcilroy, J. B. Antcliffe, and M. D. Brasier. 2011. Effaced preservation in the
776 Ediacara biota and its implications for the early macrofossil record. Palaeontology 54:607–630.
777 Liu, A. G., D McIlroy, J. J. Matthews, and M. D. Brasier. 2012. A new assemblage of juvenile
778 Ediacaran fronds from the Drook Formation, Newfoundland. Journal of the Geological Society
779 169:395–403.
780 Liu, A. G., J. J. Matthews, and D. McIlroy 2016. The Beothukis/Culmofrons problem and its
781 bearing on Ediacaran macrofossil taxonomy: evidence from an exceptional new fossil
782 locality. Palaeontology 59:45–58.
783 Magurran, A. E. 2013. Measuring biological diversity. John Wiley & Sons.
784 Mason, B., G. Kerr, A. Pommerening, et al. 2003 Continuous cover forestry in British conifer
785 forests. Forest Research Annual Report and Accounts 2004:38–53.
786 Matthews, J. J., A. G. Liu, and D. McIlroy. 2017. Post–fossilization processes and their
787 implications for understanding Ediacaran macrofossil assemblages. Geological Society, London,
788 Special Publications 448:251–269.
789 McCook, L., J. Jompa, and G. Diaz-Pulido. 2001. Competition between corals and algae on coral
790 reefs: a review of evidence and mechanisms. Coral reefs 19:400–417.

McIlroy, D. and M. Garton. 2010. Realistic interpretation of ichnofabrics and palaeoecology of the pipe- rock biotope. Lethaia 43:420–426.

Milns, I., C. M. Beale, and V. A. Smith. 2010. Revealing ecological networks using Bayesian network inference algorithms. Ecology 91:1892–1899.

Mitchell, E. G., C. G. Kenchington, A. G. Liu, J. J. Matthews, and N. J. Butterfield. 2015. Reconstructing the reproductive mode of an Ediacaran macro–organism. Nature 524: 343.

Mitchell–Olds, T., and J. Schmitt. 2006. Genetic mechanisms and evolutionary significance of natural variation in Arabidopsis. Nature 441:947.

Muko, S., I. K. Shimatani, and Y. Nozawa. 2014. Spatial analyses for non–overlapping objects with size variations and their application to coral communities. Journal of Animal Ecology 83:980–990.

Narbonne, G. M. 2004. Modular construction of early Ediacaran complex life forms. Science 305:1141–1144.

Ogg, J. G., G. Ogg, and F. M. Gradstein. 2008. The Concise Geologic Time Scale Cambridge University Press.

Raventós, J., T. Wiegand, and M. De Luis. 2010. Evidence for the spatial segregation hypothesis: a test with nine year survivorship data in a Mediterranean shrubland. Ecology 91: 2110–2120.

Seidler, T. G., and J. B. Plotkin. 2006. Seed dispersal and spatial pattern in tropical trees. PLoS Biology 4:e344.

Seilacher, A., L. A. Buatois, and M. G. Mángano. 2005. Trace fossils in the Ediacaran–Cambrian transition: behavioural diversification, ecological turnover and environmental shift. Palaeogeography, Palaeoclimatology, Palaeoecology 227:323–356.

813 Smith, C. R., A. G. Glover, T. Treude, N. D. Higgs, and D. J. Amon. 2015. Whale–fall
814 ecosystems: recent insights into ecology, paleoecology, and evolution. Annual review of marine
815 science 7:571–596.
816 Smith, V. A., J. Yu, T. V. Smulders, A. J. Hartemink, and E. D. Jarvis. 2006. Computational
817 inference of neural information flow networks. PLoS computational biology 2:e161.
818 Sobel, J. M., G. F. Chen, L. R. Watt, and D. W. Schemske. 2010. The biology of
819 speciation. Evolution 64:295–315.
820 Sperling, E. A., K. J. Peterson, and M. Laflamme. 2011. Rangeomorphs, *Thectardis* (*Porifera*?)
821 and dissolved organic carbon in the Ediacaran oceans. Geobiology 9:24–33.
822 Stachowicz, J. J. 2001. Mutualism, facilitation, and the structure of ecological communities:
823 positive interactions play a critical, but underappreciated, role in ecological communities by
824 reducing physical or biotic stresses in existing habitats and by creating new habitats on which
825 many species depend. AIBS Bulletin 51:235–246.
826 Tilman, D. 1985. The resource–ratio hypothesis of plant succession. The American
827 Naturalist 125:827–852.
828 Velázquez, E., M. Kazmierczak, and T. Wiegand. 2016. Spatial patterns of sapling mortality in a
829 moist tropical forest: consistency with total density dependent effects. Oikos 125:872–882.
830 Waggoner, B. 2003. The Ediacaran Biotas in Space and Time. Integrative and Comparative
831 Biology 43:104–113.
832 Wang, X., T. Wiegand, A. Wolf, et al. 2011. Spatial patterns of tree species richness in two
833 temperate forests. Journal of Ecology 99:1382–1393.
834 Wiegand, T., and K. A. Moloney. 2004. Rings, circles, and null- models for point pattern
835 analysis in ecology. Oikos 104:209–229.

836 Wiegand, T., and K. A. Moloney. 2013. Handbook of spatial point–pattern analysis in ecology.
837 CRC Press.
838 Wiegand, Thorsten, W. Daniel Kissling, Pablo A. Cipriotti, and Martin R. Aguiar. 2006.
839 Extending point pattern analysis for objects of finite size and irregular shape. Journal of
840 Ecology 94:825–837.
841 Wiegand, T., S. Gunatilleke, and N. Gunatilleke. 2007A. Species associations in a heterogeneous
842 Sri Lankan dipterocarp forest. The American Naturalist 170:E77–E95.
843 Wiegand, T., S. Gunatilleke, N. Gunatilleke, and T. Okuda. 2007B. Analyzing the spatial
844 structure of a Sri Lankan tree species with multiple scales of clustering. Ecology 88:3088–3102.
845 Wiegand, T., I. Martínez, and A. Huth. 2009. Recruitment in tropical tree species: revealing
846 complex spatial patterns. The American Naturalist 174:E106–E140.
847 Wiegand, T., A. Huth, S. Getzin, X. Wang, Z. Hao, C. V. S. Gunatilleke, and I. N. Gunatilleke.
848 2012. Testing the independent species' arrangement assertion made by theories of stochastic
849 geometry of biodiversity. Proceedings of the Royal Society of London B: Biological
850 Sciences:rspb 20120376.
851 Wilby, P. R., J. N. Carney, and M. P.A. Howe. 2011. A rich Ediacaran assemblage from eastern
852 Avalonia: evidence of early widespread diversity in the deep ocean. Geology 39:655–658.
853 Willis, R. Jl. 2007. The history of allelopathy. Springer Science & Business Media.
854 Wood, D. A., R. W. Dalrymple, G. M. Narbonne, J. G. Gehling, and M. E. Clapham. 2003.
855 Paleoenvironmental analysis of the late Neoproterozoic Mistaken Point and Trepassey
856 formations, south-eastern Newfoundland. Canadian Journal of Earth Sciences 40:1375–1391.

857 Yu, J., V. A. Smith, P. P. Wang, A. J. Hartemink, and E. D. Jarvis. 2004. Advances to Bayesian
858 network inference for generating causal networks from observational biological
859 data. Bioinformatics 20:3594–3603.

860 **Acknowledgements**

861 Environment and Conservation, Government of Newfoundland and Labrador provided
862 permits to conduct research within the Mistaken Point Ecological Reserve in 2010. Access to the
863 aforementioned fossil localities is by scientific research permit only. Contact the Department
864 listed above for further information. This work has been supported by the Natural Environment
865 Research Council (NE/G523539/1 and NE/P002412/1) and a Henslow Research Fellowship at
866 Murray Edwards College from the Cambridge Philosophical Society to E.G.M. We thank Alex
867 Liu and Charlotte Kenchington for discussions relating to this work and the two reviewers for
868 their helpful comments.

869

Figures and table

Correlation	Removal p-value	Direction	Mean IS	Size seen (m)	95 %	Bootstrapping 90 %	80 %	70 %	60 %	50 %
Brad-Char	0.0497	0.10	0.2990	1.50	60	54	56	48	28	29
Lob-Char	0.0002	0.06	-0.2157	0.50	57	56	59	54	51	29
Fract-Lob	0.0006	NA	0.1420	1.00	68	67	60	54	50	54
Fract-Ives	0.0046	NA	0.1719	1.75	83	69	44	42	36	32
Plum-Fract	0.0008	NA	0.0000	1.75	66	45	35	31	30	13
Disc-Fract	0.0000	0.07	0.1522	0.50	96	88	86	74	36	48
Plum-Ives	0.0000	NA	0.0021	1.00	52	49	46	42	38	19
Disc-Plum	0.0171	NA	0.1432	1.50	68	52	36	29	32	19
Chard-Plum	0.0000	NA	0.3959	0.50	63	68	71	62	61	69
Chard-Hiem	0.0011	0.01	0.0000	1.00	75	61	54	15	17	22
Plum-Other	0.0010	0.06	0.0000	1.50	94	77	69	48	42	42
Hiem-Other	0.0063	NA	0.0000	1.50	99	83	75	56	38	16
Chard-Other	0.0016	NA	0.4843	1.75	59	51	53	47	37	32
Ives-Chard	0.0001	NA	0.5016	1.75	100	71	70	50	60	67

Table 1. Edge properties for the Bayesian Network given in Figure 4. The columns are labelled as follows: Removal p-value: The p-value for whether the network score (the fit of the network onto the data) is significantly different if that correlation is removed. Direction: The p-value for whether the network score is significantly different if the direction of that correaltion is reversed. NA indicate mutual correlations. Mean IS: The mean interaction strength of all the networks bootstrapped at 95%. Size seen (m): The smallest quadrat size which the correlation is detected. 95%: The occurrence rate for the 95% bootstrapped networks which indicates consistency of correlation over different quadrats of the area of the bedding plane. Bootstrapping 90-50%: The occurances rates for the bootstrapped data when sub-sampled at the 50, 60, 70, 80 and 90% levels. The following taxa notation is used: Brad: *Bradgatia*, Char: Charniid Chard:

882 *Charniodiscus*, Plum: *Plumeropriscum*, Fract: *Fractofusus*, Hiem: *Hiemalora*, Ives:

883 Ivesheadiomorph, Lob: Lobate Discs.

884

885

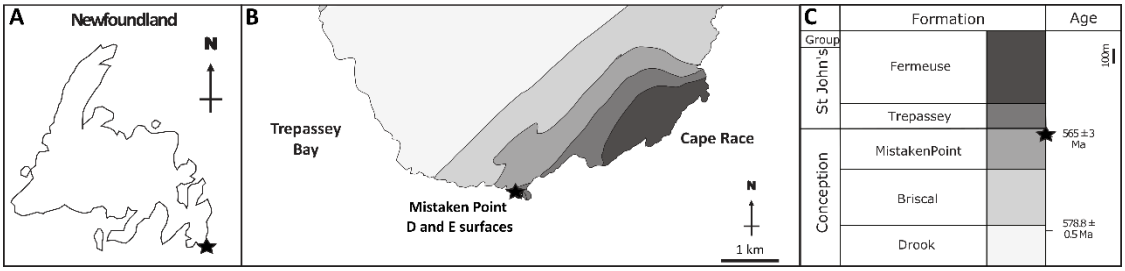

886

887 **Figure 1:** Locality showing (A) the location of Mistaken Point Ecological Reserve in

888 Newfound Canada. (B) The location of D and E surfaces within the reserve with the formations

889 shown in grey scale as given in (C). (C) Stratigraphic column showing radiometric dates and the

890 location of D and E surfaces. Modified from Liu 2016 (Fig. 1 E-F).

891

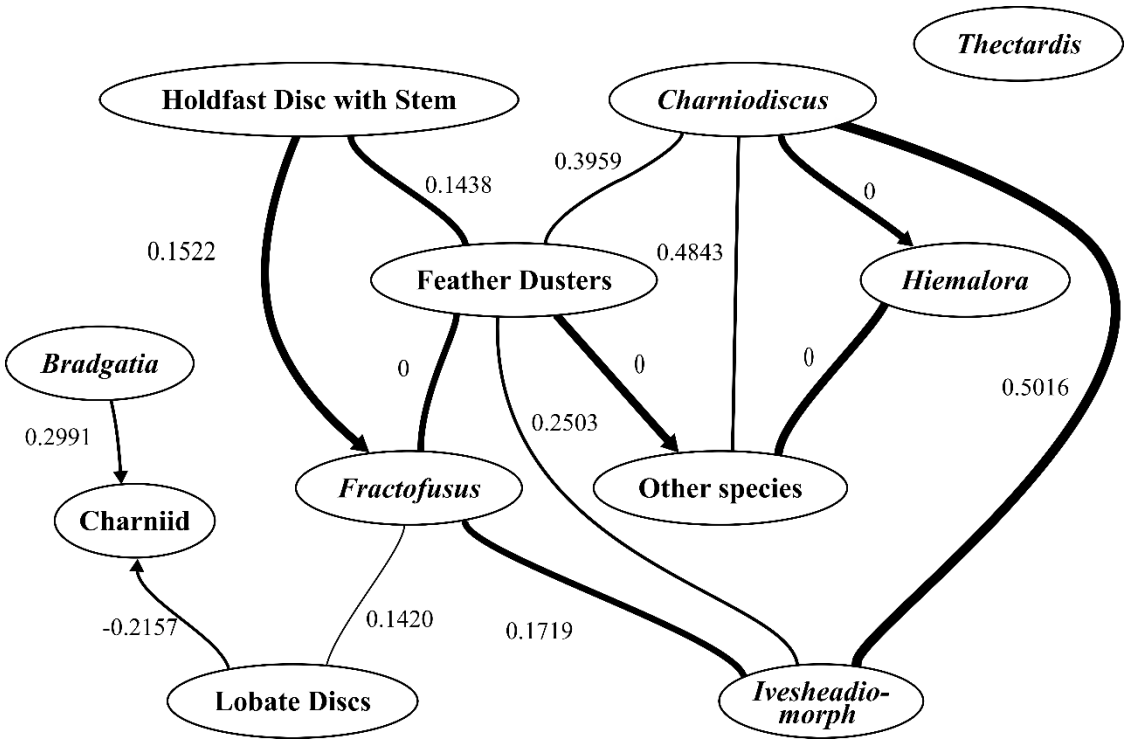

Figure 2: Bayesian Network for the 'E' surface. Correlations are indicated by lines connecting the two taxa. The occurrence rate is indicated by the width of the edge; the wider the line, the higher the occurrence rate. Arrows indicated non-mutual dependence between two taxa. Numbers by the lines are the mean interaction strengths of the correlations, with positive interaction strengths indicating aggregation, negative segregation, and zero indicating different aggregation and segregation behaviours at different densities.

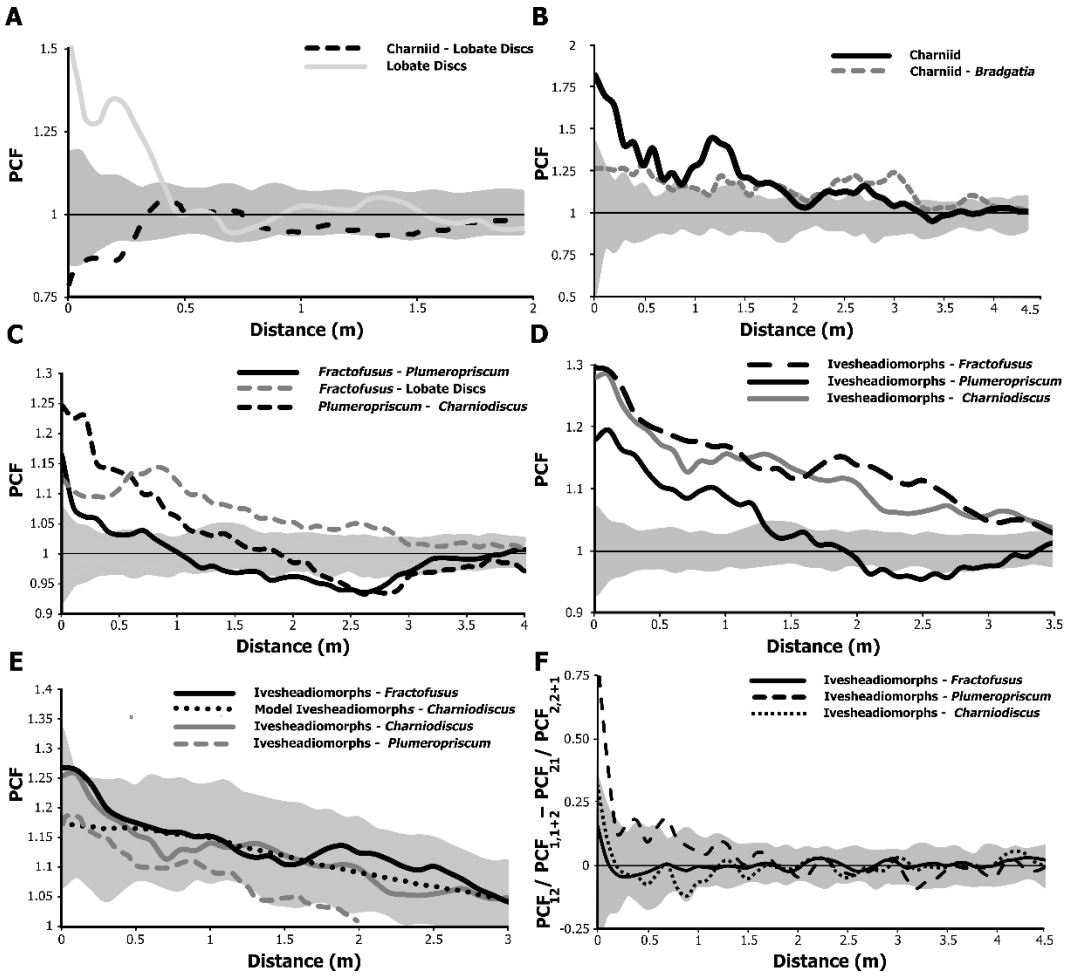

Figure 3. Pair correlation functions (PCF) for the 'E' surface. The x-axis is the inter-point distance between organisms in metres. On the y-axis, PCF = 1 indicates CSR, <1 indicates segregation and >1 indicates aggregation. (A) Charniid – Lobate Disc bivariate distribution and Lobate Disc univariate distribution. Grey shaded area is the boundaries of 99 Monte Carlo simulation of the CSR bivariate distribution. (B)) Charniid – *Bradgatia* bivariate distribution and Charniid univariate distribution. Grey shaded area is the boundaries of 99 Monte Carlo simulation of the CSR bivariate distribution.. (C) PCFs of non-Ivesheadiomorph bivariate distributions of *Fractofusus* and *Plumeropriscum*. Grey shaded area is the boundaries of 99 Monte Carlo simulation of the CSR bivariate distribution of *Fractofusus – Plumeropriscum*. (D)

910 Bivariate PCFs of Ivesheadiomorph interactions. Grey shaded area is the boundaries of 99 Monte
911 Carlo simulation of the CSR bivariate distribution of Ivesheadiormorph – *Plumeropriscum.* (E)
912 Bivariate PCFs of Ivesheadiomorph interactions showing the best-fit shared source model of
913 Ivesheadiomorph – *Charniodiscus.* Grey shaded area showing the boundaries of 99 Monte Carlo
914 simulations for the best-fit shared source model of Ivesheadiomorph – *Charniodiscus*. (F) RLA
915 results for the Ivesheadiomorph distributions. On the y-axis, PCF = 0 indicates CSR. Grey
916 shaded area is the boundaries of 99 Monte Carlo simulation of the CSR randomlly labelled
917 distributions.
918

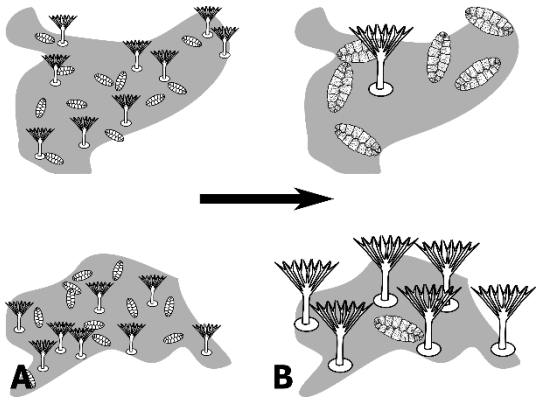

Figure 4: (A) Reconstruction of the habitat association between *Fractofusus* – *Plumeropriscum* resulting in mutual aggregation on top of the deduced heterogeneous habitat (grey). In the case of *Plumeropriscum – Fractofusus* (and *Plumeropriscum – Charniodiscus*, not figured), these habitat associations result in competition for resources between mature specimens leading to thinning (segregation) of these larger individuals (B). Note that only a single generation are depicted to ensure clarity of the process. More realistically there would be multiple generations and different size classes (since these taxa reproduce continuously, Darroch et. al. 2013).

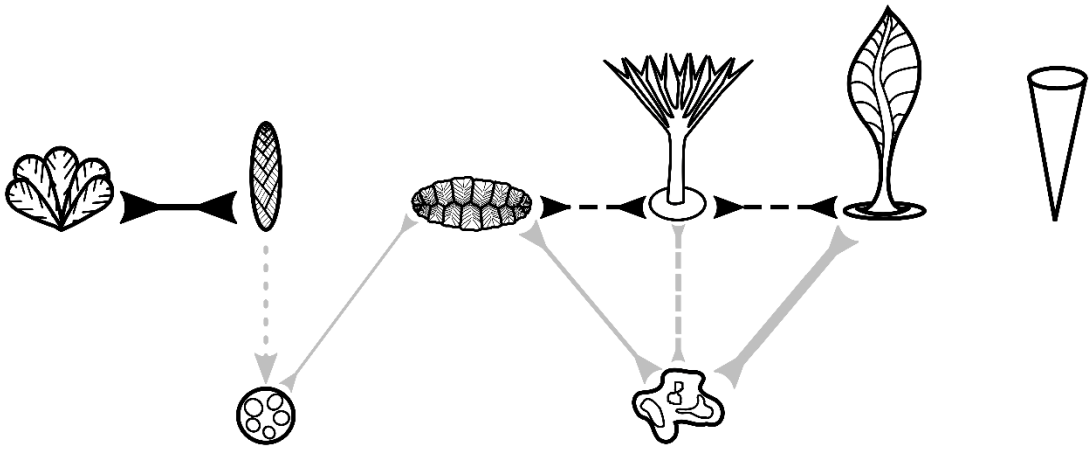

Figure 5: Summary diagram of the E surface bivariate interactions and associations. Top row: *Bradgatia*, Charniid, *Fractofusus*, *Plumeropriscum*, *Charniodiscus*, *Thectardis*. Bottom row: Lobate Discs, Ivesheadiomorphs. Grey line denote taxa with unknown/desputed affinities while black indicates interactions and associations between living-at-time-of-burial organisms. Two inward arrows indicate mutual habitat associations, solid lines indicate only these habitat associations, while long dashes indicated these associations result in resource competition. Arrow with dotted line depicts pre-emptive competition.

Taxon 1	Taxon 2	Model	Output values				
			σ (m)	Cluster Size	No. of cluster	p-value	Error
Ives	Chard	LCM	0.213	14	126	0.06	0.00079
Brad	Chard	LCM	2.742	56	13	0.33	0.00548
Ives	Plum	LCM	0.282	43	19	0.32	0.00300
Ives	Fract	LCM	0.570	34	23	0.25	0.00920
Lob	Fract	LCM	0.219	51	12	0.34	0.00394
Chard	Plum	LDCM	0.329	12	19	0.11	0.07695
Fract	Plum	LDCM	0.723	60	419	0.01	0.00417
Ives	Fract	LDCM	0.497	99	68	0.24	0.00162
Brad	**Char**	**SS**	**1.374**	**27**	**14**	**0.66**	**0.00186**
Chard	**Plum**	**SS**	**0.450**	**9**	**18**	**0.97**	**0.00168**
Fract	**Plum**	**SS**	**0.457**	**9**	**28**	**0.79**	**0.00030**
Ives	**Plum**	**SS**	**0.457**	**9**	**19**	**0.69**	**0.00036**
Ives	**Fract**	**SS**	**1.212**	**24**	**11**	**0.65**	**0.00098**
Ives	**Chard**	**SS**	**1.060**	**22**	**14**	**0.82**	**0.00016**
Lob	**Fract**	**SS**	**1.268**	**26**	**14**	**0.70**	**0.00177**

Supplementary Table S1. *Bivariate parameters for the best-fit models for the aggregated correlations.* The parameters for the shared source models (SS), linked cluster models (LCM) and linked double cluster models (LDCM). $p_d = 1$ corresponds to a perfect fit of the model on the data, while $p_d = 0$ corresponds to no fit at all. 2σ denotes the size of the cluster radius. CSR models are not included in this table because for all $p_d < 0.01$ The rows in bold are the best-fit models for those correlations. The Charniid – Lobate disc correlation is not included because it is a segregation, not aggregation. The best-fit models for each correlation are shown in bold. The following taxa notation is used: Chard: *Charniodiscus*, Plum: *Plumeropriscum*, Fract: *Fractofusus*, Ives: Ivesheadiomorph, Lob: Lobate Discs.

Correlation Modelled	Correlation compared					
	Chard - Ives	**Plum - Chard**	**Plum - Ives**	**Fract - Plum**	**Fract - Ives**	**Fract - Lob**
Chard - Ives	**0.82**	0.04	0.15	0.22	0.38	0.20
Plum - Chard	0.01	**0.97**	0.06	0.01	0.01	0.40
Plum - Ives	0.01	0.55	**0.69**	0.58	0.71	0.01
Fract - Plum	0.04	0.04	0.64	**0.79**	0.01	0.16
Fract - Ives	0.01	0.01	0.56	0.02	**0.65**	0.34
Lob - Fract	0.13	0.01	0.08	0.01	0.07	**0.82**

Supplementary Table S2. *The p-values of the best fit models fit onto other interactions*. To check for consistence of data, and the best fit models fit onto the bivariate PCFs of other correlations. A value of $p_d = 1$ corresponds to a perfect fit of the model on the data, while $p_d = 0$ corresponds to no fit. Note that while these numbers may seem low they need to be considered in context of the PCF graph (Fig. 3), which show the small fluctuations of the observed PCF around the model PCF. The following taxa notation is used: Brad: *Bradgatia*, Char: Charniid Chard: *Charniodiscus*, Plum: *Plumeropriscum*, Fract: *Fractofusus*, Ives: Ivesheadiomorph, Lob: Lobate Discs.

Taxon 1	Taxon 2	$PCF_{12}/PCF_{1,1+2} - PCF_{21}/PCF_{2,1+2}$
Fract	**Ives**	0.85
Chard	**Ives**	0.37
Plum	**Ives**	0.01

Supplementary Table S3. *P-values for random labelling analysis*. The PCF of taxon 1 is given by $PCF_{11,}$ Taxon 2 by PCF_{22} , Taxon 1 on 2 PCF_{12} , Taxon 2 on 1 PCF_{21}, Taxon 2 over the combined PCFs of both taxa $PCF_{2,1+2}$ and Taxon 1 over the combined PCFs of both taxa $PCF_{12}/ PCF_{1,1+2}$. A $p_d^{RLA} = 1$ corresponds the CSR model, and so a random RLA pattern between the two taxa - zero difference between the two groups. Therefore, where $p_d^{RLA} = 1$ there is no density dependence whereas $p_d^{RLA} = 0$ corresponds to no CSR model fit between the two groups, thus a density dependent spatial pattern. The following taxa notation is used: Chard: *Charniodiscus*, Plum: *Plumeropriscium*, Fract: *Fractofusus*, Ives: Ivesheadiomorph.

Taxon 1	Taxon 2	Taxon 1	Taxon 2	Joint 1 and 2	Radius (m)
Chard	**Ives**	0.58	0.14	0.75	0.50
Plum	**Chard**	0.01	0.01	0.02	0.70
Plum	**Ives**	0.01	0.01	0.03	0.50
Fract	**Plum**	0.01	0.01	0.01	0.60
Fract	**Ives**	0.56	0.02	0.55	0.30
Fract	**Lob**	0.07	0.02	0.03	0.50
Char	**Brad**	0.07	0.03	0.05	1.00
Char	**Lob**	0.01	0.01	0.01	0.50

Supplementary Table S4. *P-values for heterogeneous Poisson models created using the background densities of taxa given by the columns*). $p_d = 1$ corresponds to a perfect fit of the model on the data, while $p_d = 0$ corresponds to no fit at all. Radius is the radius of the kernel used to generate the heterogeneous background. The following taxa notation is used: Chard: *Charniodiscus*, Plum: *Plumeropriscum*, Fract: *Fractofusus*, Ives: Ivesheadiomorph, Lob: Lobate Discs, Char: Charniid, Brad: *Bradgatia.*

Supplementary Information

Extended methods

Specimen identification

To minimise identification errors, coarse taxonomic groups were used to (c.f. Clapham 2011). For example, subtle differences in branching structure or morphological structures that differentiate species or even genera may not be preserved, e.g. *Beothukis* and *Vinlandia* are distinguished by a single branching characteristic (Brasier et al. 2012). Identification to genus

988 level or higher order taxonomic rank is inevitably more robust to preservational variations, and is
989 standard practice in modern community ecology analysis (Milns et al. 2010).
990 By far the most dominant type of fossil preserved on the D and E surfaces are
991 rangeomorphs, a group characterized by a fractally branching morphology with unresolved
992 phylogenetic affinities. Five of the ten taxonomic groups used in this study are rangeomorphs:
993
994 1) *Bradgatia* (Fig. 3g). A frondose rangeomorph (*B. linfordensis*), with multifoliate
995 branches emanating from a common basal attachment (Boynton and Ford 1995, Flude
996 and Narbonne 2008). *Bradgatia* is the second most abundant taxon on D surface (9.9%
997 of the total assemblage, 140 specimens), but relatively rare on E surface (1.1% of the
998 total assemblage, 34 specimens). On D surface it measures 2.1-11.6 cm in long-axis
999 dimension, vs. 5.4-18.9 cm for the E surface population (Clapham et al. 2003).
1000 2) Charniids (Fig. 3a). A group of frondose rangeomorphs with primary branches
1001 alternating along a central stem, represented on D and E surfaces by *Beothukis*
1002 *mistakensis* (Brasier et al. 2009) and rare specimens of *Charnia masoni* (Ford 1958) (see
1003 Fig. 4a, b, Laflamme et al. 2007). Charniids are found on both the D and E surfaces
1004 (1.7% and 2.5% of their total assemblages, with 25 and 76 specimens respectively). On
1005 D surface their preserved long-axis dimension is 6.7-27.0 cm, vs. 2.8-21.2 cm on E
1006 surface (Clapham et al. 2003).
1007 3) *Pectinifrons* (Fig. 3e). A rangeomorph genus (*P. abyssalis*) with multiple branches
1008 arranged to one side of a central trunk (Bamforth et al. 2008). *Pectinifrons* is only found
1009 on D surface where it is one of only three abundant taxa (7.6% of the total assemblage,
1010 108 specimens); long-axis dimension 2.8-16.6cm (Clapham et al. 2003).

4) *Plumeropriscum* (Fig. 3b). A genus (*P. hofmanni*) of frondose Rangeomorphs with branches emananting from a shared point at the top of the stem (Mason and Narbonne 2016); previously known as Feather Dusters (cf. Clapham et al. 2003). *Plumeropriscum* occur abundantly on the E surface (9.1% of the assemblage, 272 specimens), with a long-axis dimension of 0.9-15.3 cm (Clapham et al. 2003).

5) *Fractofusus* (Fig. 3i). A rounded, elongate spindle-like rangeomorph, with two offset rows of irregularly alternating, self-similar, subdivided frondlets arranged along a central axis (Gehling and Narbonne 2007). *Fractofusus misra* is the most common taxon on both D and E surfaces, with limited (<5) *Fractofusus andersoni* present. *Fractofusus* comprises of 76.3% and 38.4% of the respective assemblages (1070 and 1140 specimens respectively); long-axis dimension on D surface is 0.9-113.0 cm, vs. 2.75-36.25 cm on E surface (Clapham et al. 2003).

Three further non-rangeomorph groups in this study are sufficiently distinct to recognize as bona fide biological entities:

6) *Charniodiscus* (Fig. 3c). A stalked frondose 'arboreomorph' characterized by a distinct disc-shaped holdfast and absence of fractal, rangeomorph style branching (Laflamme and Narbonne 2008, Brasier et al. 2012, Hoyal Cuthill and Conway Morris 2014). Two species of *Charniodiscus* occur abundantly on the E surface (11.0% of the total assemblage, 326 specimens) with a long-axis dimension of 1.0 - 29.1 cm (Clapham et al. 2003).

7) *Hiemalora* (Fig. 3h). A discoidal organ-taxon, distinguished by radial filaments emanating from the circumference. *Hiemalora stellaris* is often considered an organ taxon of *Primocandelabrum hiemaloranum* (Hoffmann et al. 2008). Hiemalora comprises 1.3% of specimens on E surface (39 specimens), with a disc diameter of 0.8-2.7 cm (Clapham et al. 2003).

8) *Thectardis* (Fig. 3d). A triangular shaped fossil, with conspicuously limited morphological distinction and much-debated phylogenetic affinity (e.g. Narbonne et al. 2014); one possibility is that it is a sponge (Sperling et al. 2011). *Thectardis* is found exclusively on the E surface (1.3% of the total assemblage, 39 specimens), and has a long-axis dimension of 4.8-16.5cm (Clapham et al. 2003).

The final two groupings used in this analysis are the degradationally obscured remains of one or more pre-existing forms (taphomorphs). They are included because of their numerical abundance on both of the analysed surfaces, and the likelihood that their distribution had some correspondence to overall community structure. The two taphomorph groups are:

9) Lobate Discs (Fig. 3f). A group of putative taphomorphs characterized by a circular shape, with high relief, approximately radially symmetrical, irregular lobes. Lobate discs have been suggested to be the taphomorphs of holdfast discs (Liu et al. 2011). Lobate discs are found on the E surface, (5.4% of the total assemblage, 160 specimens) with a diameter range of 3.6-38.4cm (Clapham et al. 2003).

10) Ivesheadiomorphs (Fig. 3j). A group of putative taphomorphs characterized by a lack of consistent internal or external form, low preservation detail and rarity of symmetrical features (Liu et al. 2011). The precursor taxa from which they decayed is unknown, but likely to vary. 25 specimens were documented on D surface (1.8% of the total biota. On the E surface form 7.9% of the total assemblage (232 specimens) where their dimensions range from 5.5-55.0cm (Clapham et al. 2003).

In addition to these ten more or less recognizable 'taxa' we identify two further bins. The first includes frondose organisms that are too eroded/degraded to identify while the second is to accommodate forms representing less than 1% of their respective biotas (< 30 specimens on D surface, or <50 specimens on E Surface) and/or are cannot be placed in a known 'taxon'.

11) "Holdfast Discs" is a bin-group that includes all discoidal specimens of uncertain affinity, with or without associated stems, which lack sufficient preservation detail to identify the taxon or group. This group likely contains eroded *Charniodiscus* and *Plumeropriscum* specimens (c.f. the frondose group of Clapham et al. 2003). This bin group forms a large proportion of specimens on the E surface (18.1% of the total assemblage, 530 specimens) with a long-axis dimension of 0.6-18.4cm (Clapham et al. 2003).

12) "Other species" is a bin group used to incorporate any forms that do not fall into any of the other groups. This group contains a taxonomically eclectic selection of taxa, and so does not enter into our ecological discussions - it is included here so that all documented

specimens are categorized. Of the total recorded specimens on the D surface, 1.7% fell into this category, and on the E surface 3.9% of the total assemblage, 116 specimens.

When referring to the grouped data, the groups are treated as nouns and therefore capitalized, while the taxonomic group is not e.g. Charniid is the data group that contains charniid specimens, similarly, Ivesheadiomorphs is the data group that contains ivesheadiomorph specimens. The name of the group e.g. Lobate Discs is plural, whereas for taxonomically defined species such as Fractofusus it is singular**.**

Spatial analyses

Spatial analyses fall into two broad categories: A) Bayesian network inference (BNI) and B) Spatial point process analyses (SPPA). BNI is used to identify primary correlations between taxa and SPPA is used to deduce the most likely underlying processes. Within the SPPA analyses there are three types of analysis used to determine the most likely underlying processes: B.1) description of spatial pattern using pair correlation functions (PCFs); B.2) model fitting and B.3) random labelling analyses.

A) Bayesian Network inference. – For these networks, taxa are defined as the nodes and their relationships between taxa are edges, with edge strength assigned a weighting described as the influence score (Yu et al. 2004). An influence score of one indicates a positive correlation and an influence score of minus one corresponds to a negative correlation, whereas an influence score of zero corresponds to a non-monotonic interaction (that is one that has different behaviour at different spatial scales).

1099 Banjo requires discrete data, which ensures data noise is masked and only the relative
1100 densities of each taxon are important. To convert the spatial positions of specimens into data
1101 suitable for BNI analyses the following steps were taken (following Milns et al. 2010):
1102
1103 1. *Node definition.* The nodes were defined by taxa groups (Fig. 3).
1104 2. *Quadrat selection*. Abundance data was calculated in terms of specimen density within
1105 quadrats (0.25m - 2.0m) to capture different correlations at different spatial scales.
1106 3. *Discretisation*. For each quadrat, taxon density was split into three intervals: zero counts,
1107 low counts (under the median) and high counts (above the median) to capture the
1108 maximal amount of data information while masking noise (Yu et al. 2004). Zero was
1109 treated as a separate entity because the presence of one individual is very different to a
1110 zero presence (Yu et al. 2004). Medians were used in preference to means because for
1111 some groups the high counts were very high, which would result in a very small number
1112 of samples, grouped in the highest interval.
1113 4. *Contingency test filtering*. To exclude false positive correlations between taxa we used
1114 contingency filtering (χ^2 tests, $p > 0.25$).
1115
1116 This discretised data and excluded correlations were input into the BNI algorithm Banjo,
1117 which finds the best-fit network using a simulated annealing search repeated 100 million times
1118 (Heckerman et al. 1999). To minimise outliers bias, 100 samples were bootstrapped at 95% level
1119 (Magurran 2013), and each sample was analysed using Banjo. For each possible edge the
1120 probability of occurrence was bimodal, suggesting two groups of edges, the rare/low occurrence
1121 ones, and the high occurrence edges. The high occurrence edges were taken to be the

1122 constituents of the underlying network and found using Mclust (Fraley et al. 2012). The strength
1123 of each edge was calculated by finding the mean influence score of that edge over the 100
1124 sample networks.
1125 The bootstrapping performed at 95% levels was a good approximation of the data;
1126 however, by using bootstrap levels of lower percentages it was possible to compare the effect of
1127 lower taxa densities on the identified network. This enables the comparison of the likelihood of
1128 finding a correlation between taxa given variations in specimen density, for example to compare
1129 surfaces with different levels of erosion. Bootstrapped networks were found using five different
1130 bootstrap levels: 10% intervals from 90% to 50% level. For example, the average density of 'D'
1131 surface is approximately half the density of 'E' surface, due in part to higher levels of erosion
1132 (Wood et al. 2003). This density difference means that it is not clear whether any inter-surface
1133 differences are due to differences in present fossil density, or to original ecological processes.
1134 By using a 50% bootstrap level on the E surface, specimen density is similar to D surface, so
1135 more equal comparisons can be made about the inter-taxa correlation.
1136 In order to assess the effects of differential erosion between the two bedding surfaces,
1137 further BNI analyses were carried out on bootstrapped data sampled at 50%, 60%, 70%, 80% and
1138 90%. Comparison of the resultant networks was used to assess which inter-specific correlations
1139 are sensitive to density reductions, and whether lower density levels preclude finding significant
1140 correlations.
1141 Further analyses were performed to compare the effects of taxon removal, edge removal
1142 and changing edge direction to assess each of their relative importance to the network. Mann-
1143 Whitney tests were used to compare the network scores of the missing taxa networks to the
1144 networks for all taxa. If the network scores were significantly different, the taxon was said to be

1145 crucial for the network. This process was repeated for each taxon in turn. The importance of each
1146 edge was assessed in a similar way, and each edge direction was similarly assessed.
1147 *B) Spatial point process analyses*. – Differential erosion has the potential to distort spatial
1148 analyses (Matthews et al. 2017) and this data has been tested for impact of differential erosion
1149 using heterogeneous Poisson models to model possible sources of erosion (Mitchell et al. 2015),
1150 with no significant effects found.
1151
1152 *B.1) Bivariate PCFs* were calculated from the population density using a grid of 10cm x
1153 10cm cells. To minimise noise a smoothing was applied to the PCF dependent on specimen
1154 abundance: A three cell smoothing over this grid was applied for *Fractofusus,* five cells for
1155 *Charniodiscus*, Ivesheadiomorph and *Plumeropriscum* s*,* and 15 cells for *Bradgatia* and
1156 Charniid. To test whether the PCF exhibited complete spatial randomness (CSR), 99 simulations
1157 were run for each relationship on a homogeneous background to generate simulation envelopes
1158 around the random (PCF = 1) and the fit of the fossil data to CSR was done using Diggle's
1159 goodness-of-fit test (p_d, Diggle 2003, Illian et al. 2008). Note that due to non-independence of
1160 spatial data, Monte-Carlo generated simulation envelopes cannot be interpreted as confidence
1161 intervals.
1162 Additionally, these two comparisons should be used in tandem for the following reasons:
1163 1) the Monte Carlo simulation envelopes do not necessarily correspond to confidence intervals,
1164 and run the risk of Type I errors if the observed PCF falls near the edge of the simulation
1165 envelope (Illian et al. 2009). 2) The p_d does not strictly test whether a model should be accepted
1166 or rejected, but whether the PCFs for the observed data are within the range of the stochastic
1167 realization of the model (Diggle 2003). 3) The p_d depends on the range over which it is

calculated. For example, the model may not fit at very small distances due to the physical occupation of that space by the organisms themselves, but fit well at larger distances (Diggle 2003; Illian et al. 2008). Thus, visual inspection of the PCFs with Monte Carlo simulation envelopes, coupled with p_d ensures that these errors are minimzed.

B.2) *Aggregation model fitting.* For each bivariate aggregation found, the fit of heterogeneous Poisson models, shared source models, linked cluster and linked double cluster models were compared to the observed data following the same procedure as for testing for CSR (Baddeley et al. 2015).

Heterogeneous Poisson models. – Heterogeneous models were fit to each bivariate interaction, and their fit assessed using 99 Monte Carlo simulations and p_d-values. Three different heterogeneous backgrounds were generated from density maps of taxa defined by a circle of radius r over which the density is averaged throughout the mapped fossiliferous surface area. Density maps were formed using estimators within the range of $0.1 < r < 1$m, and the radius corresponding to the best-fit model was used. These maps were generated for 1) taxon 1; 2) taxon 2; and 3) both taxa.

Linked and double cluster and shared source models. – Linked cluster, double cluster and shared source models were fitted to the PCF of the data. Where necessary to aid model fitting, individual taxon aggregation parameters were input. The model was checked using 99 Monte Carlo simulations, p_d-values, and by model parameter comparisons.

To assess whether each relationship could be similarly modelled by the other best-fit model from other relationships, the best-fit model from each relationship was fitted to the other

1191 relationships. Simulation envelopes and p_d-values were used to evaluate fit (SI: Table 2). To
1192 further verify these results, the best-fit models were also compared to the bivariate PCF found
1193 using Clapham et al.'s data and vice-a-versa.
1194
1195 *B.3) Random labelling analyses.* – The pattern of dead specimens within their living
1196 population can be investigated using a type of SPPA called random labelling analyses (RLA),
1197 which allows the assessment of how one sub-group behave in reference to another by randomly
1198 reassigning the identity of these sub-groups within the population. For example, when
1199 investigating the spatial patterns of dead trees within a forest, the tree position stay fixed, but
1200 whether the specimen is dead or alive is varied (De La Cruz et al. 2008). If such reassignment
1201 does not produce a significantly different spatial distribution, then the two groups have a random
1202 structure within the total spatial structure, and thus do not interact. In particular, a variant of
1203 RLA (see below) can used to detect density-dependent mortality. If this RLA reveals a
1204 significantly non-random structure, then that one group (e.g. dead specimens) is mainly located
1205 in areas with a high density of both groups (e.g. both living and dead specimens). In this case,
1206 RLA can be used to deduce whether dead trees are randomly distributed within the living, i.e.
1207 independent of the living, or whether there is a differential spatial distribution to mortality, such
1208 as localized disease (Yu et al. 2009).
1209 The PCF for each taxon (denoted PCF_{11} for taxon 1 and PCF_{22} for taxon 2), between
1210 both taxon (PCF_{12} and PCF_{12}) and over the joint pattern ($PCF_{1,1+2}$ and $PCF_{2,2+1}$) were
1211 calculated, and used to calculate the difference $PCF_{12} / PCF_{1,1+2} - PCF_{21} / PCF_{2,2+1}$. If $PCF_{12} /$
1212 $PCF_{1,1+2} - PCF_{21} / PCF_{2,2+1} > 0$ then taxon 2 are mainly located in areas with high intensity of the
1213 joint pattern and taxon 1 are in low density areas: taxon 2 have more neighbours than taxon 1.

Departure means that the process that assigns the labels is density dependent; for example, disease more easily in high density areas. These RLA differences are calculated and plotted simiarilry to PCF plots, and then the goodness-of-fit

99 Monte Carlo simulations were run where the location of both taxa remained constant, but the taxon at each specimen location were assigned randomly, and CSR assessed using these simulations and p_d value.

References unique to this section

Boynton, H. E., and T. D. Ford. 1995. Ediacaran fossils from the Precambrian (Charnian Supergroup) of Charnwood Forest, Leicestershire, England. Mercian Geologist 4:165 – 182.

Clapham, M. E. 2011. Ordination methods and the evaluation of Ediacaran communities. *In* Quantifying the Evolution of Early life, pp. 3 – 21. Springer Netherlands, 2011.

Flude, L. I., and G. M. Narbonne. 2008. Taphonomy and ontogeny of a multibranched Ediacaran fossil: Bradgatia from the Avalon Peninsula of Newfoundland. Canadian Journal of Earth Sciences 45: 1095 – 1109.

Ford, T. D. 1985. Pre – Cambrian fossils from Charnwood forest. In Proceedings of the Yorkshire Geological and Polytechnic Society 31, pp. 211 – 217. Geological Society of London.

Fraley, C., A. E. Raftery, and L. Scrucca. 2012. Normal mixture modeling for model – based clustering, classification, and density estimation. Department of Statistics, University of Washington 23:2012.

Gehling, J. G., and G. M. Narbonne. 2007. Spindle – shaped Ediacara fossils from the Mistaken Point assemblage, Avalon Zone, Newfoundland. Canadian Journal of Earth Sciences 44:367 – 387.

Laflamme, Marc., Guy M. Narbonne, and Michael M. Anderson. 2004. Morphometric analysis of the Ediacaran frond Charniodiscus from the Mistaken Point Formation, Newfoundland. *Journal of Paleontology* 78: 827 – 837.

Laflamme, M., G. M. Narbonne, C. Greentree, and M. M. Anderson. 2007.Morphology and taphonomy of an Ediacaran frond: Charnia from the Avalon Peninsula of Newfoundland. *Geological Society, London, Special Publications* 286: 237 – 257.

Narbonne, Guy M., Marc Laflamme, Peter W. Trusler, Robert W. Dalrymple, and Carolyn Greentree. 2014. Deep -water Ediacaran fossils from northwestern Canada: taphonomy, ecology, and evolution. *Journal of Paleontology* 88: 207 – 223.

Yu, Hong, Thorsten Wiegand, Xiaohui Yang, and Longjun Ci. 2009. The impact of fire and density – dependent mortality on the spatial patterns of a pine forest in the Hulun Buir sandland, Inner Mongolia, China. *Forest Ecology and Management* 257: 2098 – 2107.

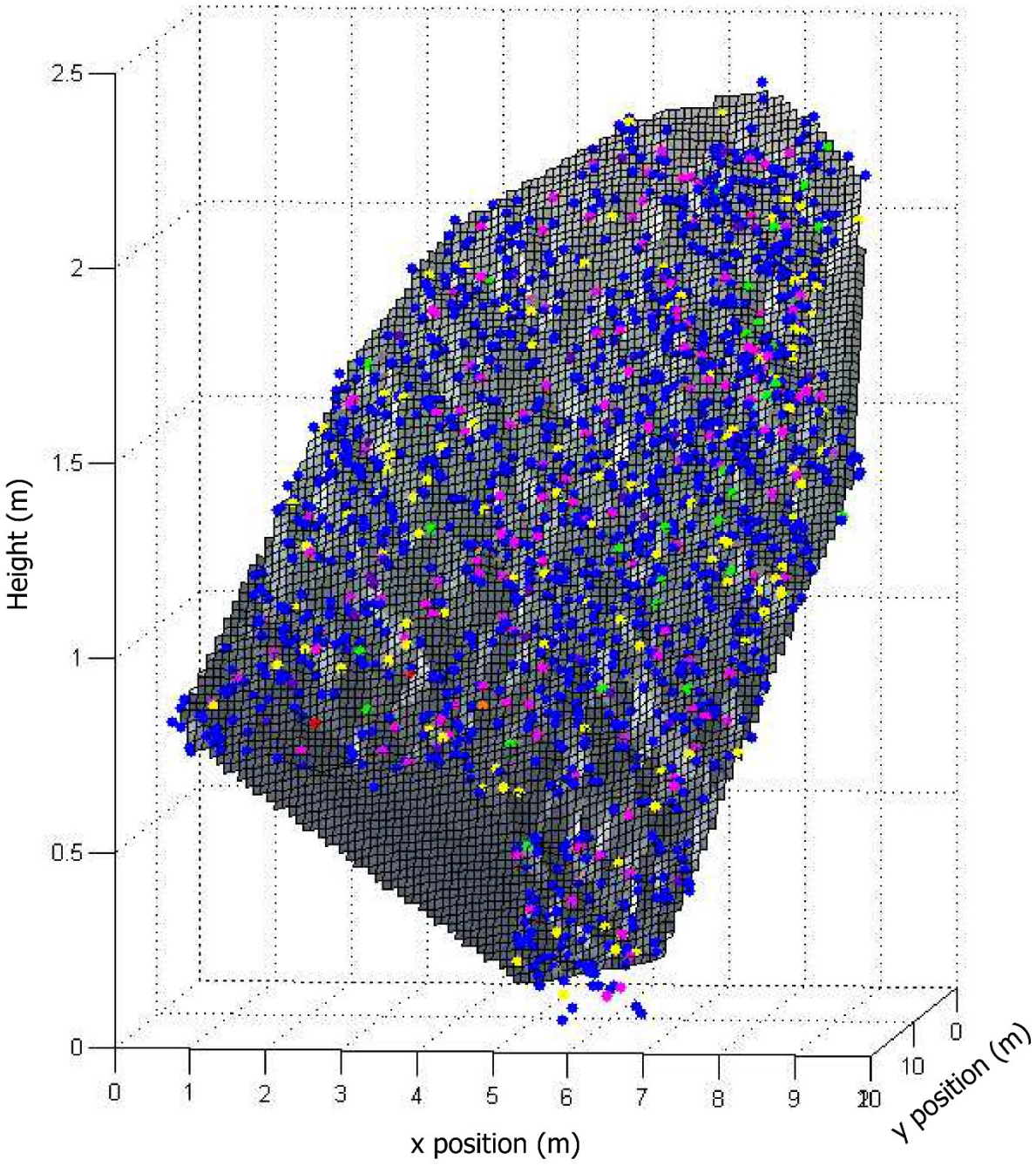
2.5
2
1.5
1
0.5
0
Height (m)
0
1
2
3
4
5
6
7
8
9
10
x position (m)
0
10
y position (m)

1249

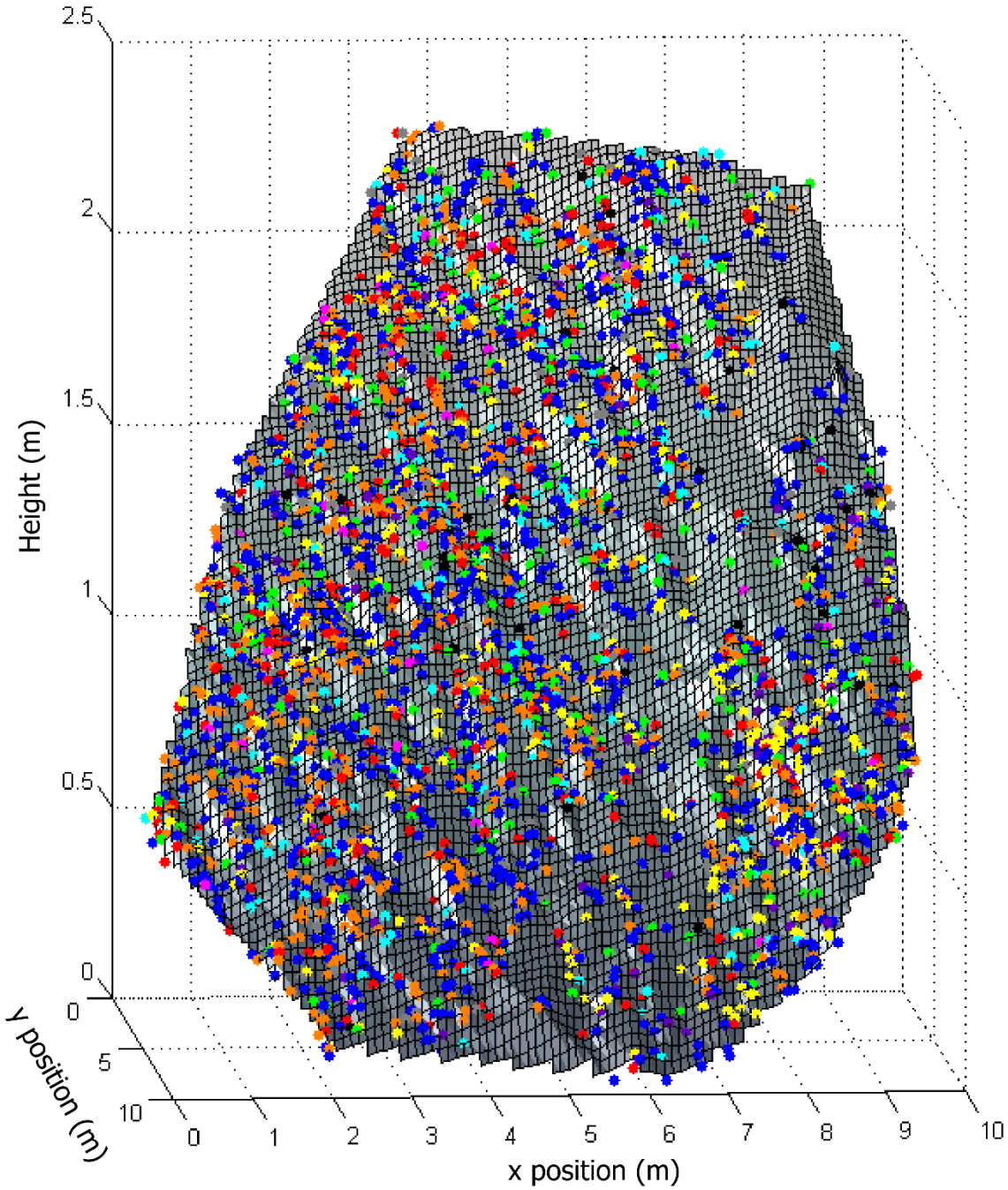

1250

1251 **Supplementary Figure 1.** Reconstruction of Bedding Planes (A) D and (B) E from mapped

1252 fossil data. The fossils are labelled as Dark Blue: *Fractofusus*, Pink: *Bradgatia*, Red:

Charniodiscus, Orange: Discs, Yellow (E surface): *Plumeropriscum*, (D surface) *Pectinifrons*, Purple: Charniid, Black: *Thectardis*, Light Blue: Lobate Discs, Green: Ivesheadiomorph, Grey: Others. Axis units are in metres.

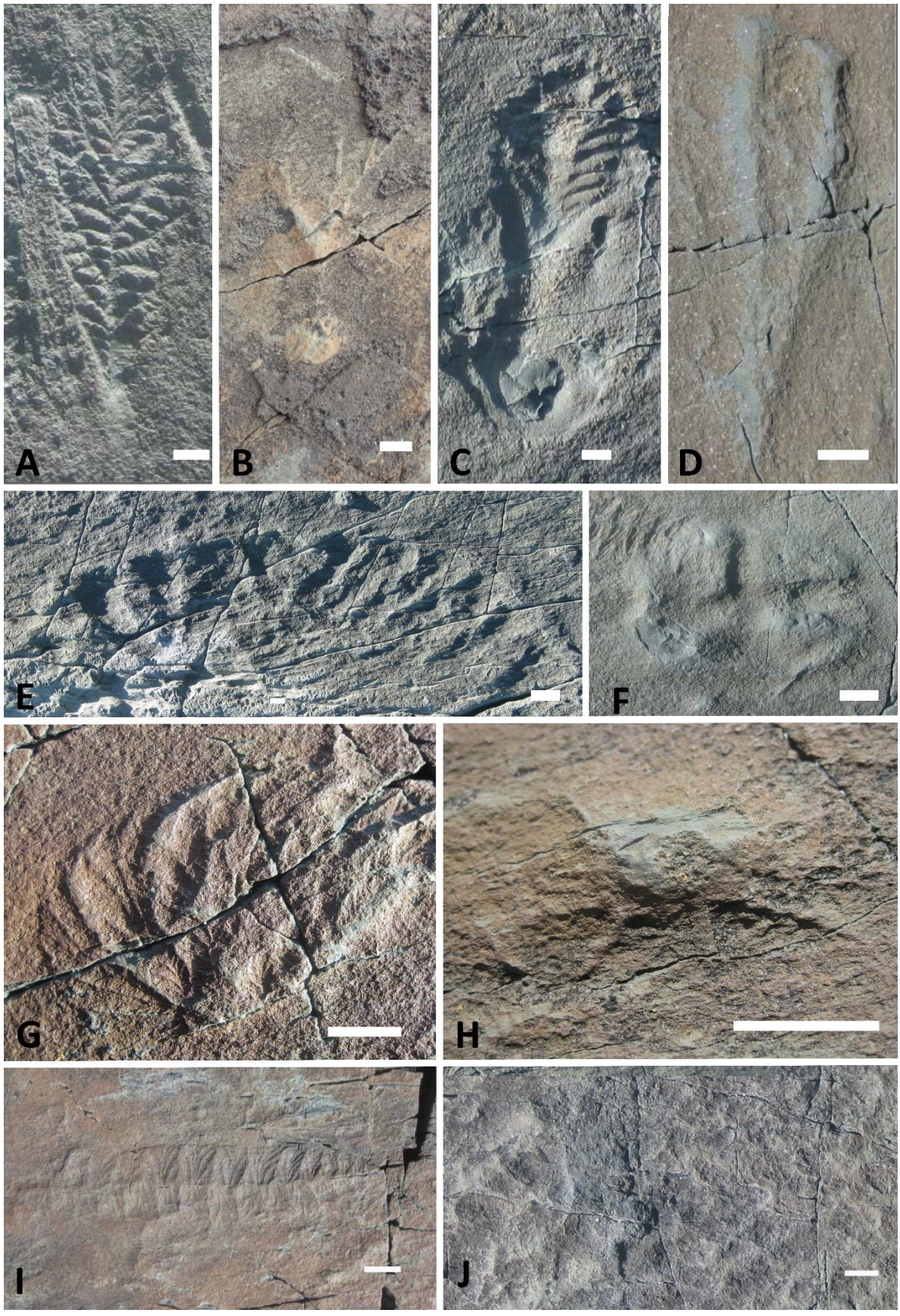
A
B
C
D
E
F
G
H
I
J

Supplementary Figure 2: Taxa of Mistaken Point 'E' Surface. Specimens were recorded as one of twelve taxonomic groups of macrofossils, (A) Charniid (*Beothukis* figured), (B) *Plumeropriscum* (C) *Charniodiscus*, (D) *Thectardis*, (E) *Pectinifrons*, (F) Lobate Discs, (G) *Bradgatia*, (H) *Hiemalora,* (I) *Fractofusus* and (J) Ivesheadiomorphs. Scale bar is 1cm. The two bin-groups are not figured because by definition they consist of irregular group of specimens.

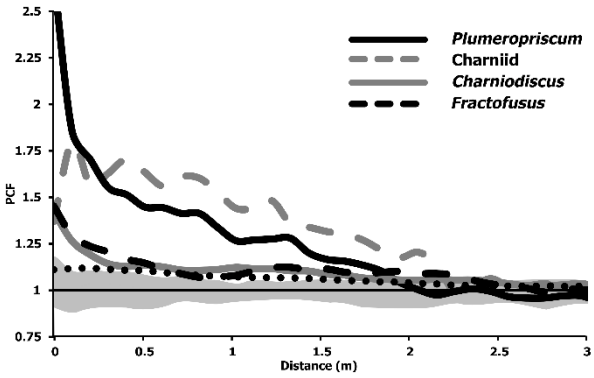

Supplementary Figure S3: Pair correlation functions (PCF) for the 'E' surface non-CSR single taxon PCFs. The x-axis is the inter-point distance between organisms in metres. On the y-axis, PCF = 1 indicates CSR, <1 indicates segregation and >1 indicates aggregation. The grey shaded area denotes the boundaries of 99 Monte Carlo simulations of CSR.